Behavioral/Systems/Cognitive

# Contribution of Dopamine D1 and D2 Receptors to Amygdala Activity in Human

**Hidehiko Takahashi,[1,3] Harumasa Takano,[1] Fumitoshi Kodaka,[1] Ryosuke Arakawa,[1] Makiko Yamada,[1] Tatsui Otsuka,[1] Yoshiyuki Hirano,[2] Hideyuki Kikyo,[1] Yoshiro Okubo,[4] Motoichiro Kato,[5] Takayuki Obata,[2] Hiroshi Ito,[1] and Tetsuya Suhara[1]**

Departments of [1]Molecular Neuroimaging and [2]Biophysics, Molecular Imaging Center, National Institute of Radiological Sciences, Chiba 263-8555 Japan, [3]Precursory Research for Embryonic Science and Technology, Japan Science and Technology Agency, Saitama, 332-0012, Japan, [4]Department of Neuropsychiatry, Nippon Medical School, Tokyo 113-8603, Japan, and [5]Department of Neuropsychiatry, Keio University School of Medicine, Tokyo 160-8582, Japan

**Several animal studies have demonstrated functional roles of dopamine (DA) D1 and D2 receptors in amygdala activity. However, the contribution of DA D1 and D2 receptors to amygdala response induced by affective stimuli in human is unknown. To investigate the contribution of DA receptor subtypes to amygdala reactivity in human, we conducted a multimodal *in vivo* neuroimaging study in which DA D1 and D2 receptor bindings in the amygdala were measured with positron emission tomography (PET), and amygdala response induced by fearful faces was assessed by functional magnetic resonance imaging (fMRI) in healthy volunteers. We used multimodality voxelwise correlation analysis between fMRI signal and DA receptor binding measured by PET. DA D1 binding in the amygdala was positively correlated with amygdala signal change in response to fearful faces, but DA D2 binding in the amygdala was not related to amygdala signal change. DA D1 receptors might play a major role in enhancing amygdala response when sensory inputs are affective.**

## Introduction

The amygdala plays a central role in processing affective stimuli, and in particular, threatening stimuli in the brain (LeDoux, 2000). The amygdala receives a moderate innervation of dopaminergic fibers (Asan, 1998), and both dopamine (DA) D1 and D2 receptors are expressed in this region (Ito et al., 2008), although the latter exhibit lower expression (Scibilia et al., 1992). DA release in the amygdala is increased in response to stress (Inglis and Moghaddam, 1999). It has been shown in animal studies that DA potentiates the response of the amygdala by augmenting excitatory sensory input and attenuating inhibitory prefrontal input to the amygdala (Rosenkranz and Grace, 2002). Systemic and local applications into the amygdala of D1 agonist and antagonist are known to potentiate and decrease fear response in animals, respectively. Although some studies reported that applications of D2 agonist and antagonist induced similar effects, the results were less consistent compared with D1-mediated effects (for review, see Pezze and Feldon, 2004; de la Mora et al., 2009).

A human functional magnetic resonance imaging (fMRI) study reported that doparminergic drug therapy such as levodopa or DA agonists partially restored amygdala response due to emotional task in Parkinson's disease patients who showed no significant amygdala response during drug-off states (Tessitore et al., 2002). In addition, another fMRI study of healthy volunteers has demonstrated that amphetamine potentiated the response of the amygdala during an emotional task (Hariri et al., 2002). More recently, Kienast et al. (2008) reported that dopamine storage capacity in human amygdala, measured with 6-[$^{18}$F]fluoro-L-DOPA positron emission tomography (PET), was positively correlated with functional magnetic resonance imaging (fMRI) signal changes in amygdala. However, the contribution of DA D1 and D2 receptors to amygdala response induced by affective stimuli is unknown in human. To investigate the relation between amygdala reactivity and dopamine receptor subtype, we conducted a multimodal *in vivo* neuroimaging study in which DA D1 and D2 receptor bindings in the amygdala were measured with PET, and amygdala response by novel faces with either neutral or fearful expression was assessed with fMRI. Based on animal pharmacological studies, we hypothesized that D1, but not D2 receptors, would predict amygdala response.

Received Nov. 17, 2009; revised Jan. 8, 2010; accepted Jan. 8, 2010.

This study was supported by a consignment expense for Molecular Imaging Program on "Research Base for PET Diagnosis" from the Ministry of Education, Culture, Sports, Science and Technology. Takanori Kochiyama and Yoko Ikoma are greatly acknowledged for her comments. We thank K. Tanimoto and T. Shiraishi for their assistance in performing the PET experiments at the National Institute of Radiological Sciences. We also thank Y. Fukushima, K. Suzuki, and I. Izumida of the National Institute of Radiological Sciences for their help as clinical research coordinators.

Correspondence should be addressed to Hidehiko Takahashi, Department of Molecular Neuroimaging, National Institute of Radiological Sciences, 9-1, 4-chome, Anagawa, Inage-ku, Chiba, Chiba 263-8555, Japan. E-mail: hidehiko@nirs.go.jp.

DOI:10.1523/JNEUROSCI.5689-09.2010

 0270-6474/10/303043-05$15.00/0

## Materials and Methods

### *Subjects*

Twenty-one male volunteers [mean age 23.1 ± (SD) 3.6 years] were studied. They did not meet the criteria for any psychiatric disorder based on unstructured psychiatric screening interviews. None of the controls were taking alcohol at the time, nor did they have a history of psychiatric disorder, significant physical illness, head injury, neurological disorder, or alcohol or drug dependence. All subjects were right-handed according to the Edinburgh Handedness Inventory. All subjects underwent MRI to rule out cerebral anatomic abnormalities. After complete explanation of the study,

written informed consent was obtained from all subjects, and the study was approved by the Ethics and Radiation Safety Committee of the National Institute of Radiological Sciences, Chiba, Japan.

*fMRI procedure*

Stimulus materials were taken from the Karolinska Directed Emotional Faces (KDEF) (Lundqvist et al., 1998). Thirty neutral and 30 fear faces were used, with half of them being male faces. The pictures were projected via a computer and a telephoto lens onto a screen mounted on a head-coil. The experimental design consisted of 5 blocks for each of the 2 conditions (neutral, fear) interleaved with 21 s rest periods. The order of presentation for the 2 conditions (neutral and fear) was randomized. During the baseline condition, subjects viewed a crosshair pattern projected to the center of the screen. In each 21 s block, 6 different faces of the same emotional class were presented for 3.5 s each. During the scans, the subjects were instructed to judge the gender of each face using selection buttons.

*fMRI scanning*

The images were acquired with a 3.0 Tesla Excite system (General Electric). Functional images of 126 volumes were acquired with T2*-weighted gradient echo planar imaging sequences sensitive to the blood oxygenation level-dependent (BOLD) contrast. Each volume consisted of 40 transaxial contiguous slices with a slice thickness of 3 mm to cover almost the whole brain (flip angle, 90°; echo time, 50 ms; repetition time, 3500 ms; matrix, 64 × 64; field of view, 24 × 24 cm).

*Analysis of fMRI data*

Data analysis was performed with the statistical parametric mapping software package (SPM2) (Wellcome Department of Cognitive Neurology, London, UK) running with MATLAB (MathWorks). All volumes were realigned to the first volume of each session to correct for subject motion and were spatially normalized to the standard space defined by the Montreal Neurological Institute (MNI) template. After normalization, all scans had a resolution of $2 \times 2 \times 2$ mm$^3$. Functional images were spatially smoothed with a three-dimensional isotropic Gaussian kernel (full-width at half-maximum of 8 mm). Low-frequency noise was removed by applying a high-pass filter (cutoff period = 128 s) to the fMRI time series at each voxel. A temporal smoothing function was applied to the fMRI time series to enhance the temporal signal-to-noise ratio. Significant hemodynamic changes for each condition were examined using the general linear model with boxcar functions convolved with a hemodynamic response function. Statistical parametric maps for each contrast of *t*-statistic were calculated on a voxel-by-voxel basis.

We assessed the contrasts of fear and neutral minus baseline (F&N-B). A random effects model, which estimates the error variance for each condition across the subjects, was implemented for group analysis. The contrast images were obtained from single-subject analysis and entered into the group analysis. A one-sample *t* test was applied to determine group response for each effect. Significant amygdala activations were identified if they reached the extent threshold of $p < 0.05$ corrected for multiple comparisons, with a height threshold of $p < 0.001$, uncorrected.

*PET scanning*

After the fMRI session, each participant underwent PET scanning. The interval between fMRI session and PET scan was 3–5 h. PET studies were performed on ECAT EXACT HR+ (CTI-Siemens). The system provides 63 planes and a 15.5 cm field of view. To minimize head movement, a head fixation device (Fixster) was used. A transmission scan for attenuation correction was performed using a germanium 68–gallium 68 source. Acquisitions were done in three-dimensional mode with the interplane septa retracted. For evaluation of D1 receptors, a bolus of 219.7 ± 6.9 MBq of [$^{11}$C]SCH23390 with specific radioactivities (95.7 ± 35.5 GBq/$\mu$mol) was injected intravenously from the antecubital vein with a 20 ml saline flush. For evaluation of extrastriatal DA D2 receptors, a bolus of 218.1 ± 14.7 MBq of [$^{11}$C]FLB457 with high specific radioactivities (221.6 ± 94.9 GBq/$\mu$mol) was injected in the same way. Dynamic scans were performed for 60 min for [$^{11}$C]SCH23390 and 90 min for [$^{11}$C]FLB457 immediately after the injection. All emission scans were reconstructed with a Hanning filter cutoff frequency of 0.4 (full-width at half-maximum, 7.5 mm). MRI was performed on Gyroscan NT (Philips Medical Systems) (1.5 T). T1-weighted images of the brain were obtained for all subjects. Scan parameters were 1-mm-thick, three-dimensional T1 images with a transverse plane (repetition time/echo time, 19/10 ms; flip angle, 30°; scan matrix, 256 × 256 pixels; field of view, 256 × 256 mm; and number of excitations, 1).

*Quantification of DA D1 and D2 receptors*

Quantitative analysis was performed using the three-parameter simplified reference tissue model (Lammertsma and Hume, 1996; Olsson et al., 1999). The cerebellum was used as a reference region because it has been shown to be almost devoid of DA D1 and D2 receptors (Farde et al., 1987; Olsson et al., 1999; Suhara et al., 1999). The model provides an estimation of the binding potential ($BP_{ND\ (nondisplaceable)}$) (Innis et al., 2007), which is defined by the following equation: $BP_{ND} = k_3/k_4 = f_2 B_{max}/\{K_d [1 + \Sigma_i F_i/K_{di}]\}$, where $k_3$ and $k_4$ describe the bidirectional exchange of tracer between the free compartment and the compartment representing specific binding, $f_2$ is the "free fraction" of nonspecifically bound radioligand in brain, $B_{max}$ is the receptor density, $K_d$ is the equilibrium dissociation constant for the radioligand, and $F_i$ and $K_{di}$ are the free concentration and dissociation constant of competing ligands, respectively (Lammertsma and Hume, 1996). Tissue concentrations of the radioactivities of [$^{11}$C]SCH23390 and [$^{11}$C]FLB457 were obtained from regions of interest (ROIs) defined on PET images of summated activity for 60 min and 90 min, respectively, with reference to the individual MRIs coregistered on summated PET images and the brain atlas. Given our hypothesis of amygdala activation during viewing novel neutral and fearful faces, ROIs were set on the bilateral amygdala. The method for defining the boundaries of the amygdala was adapted from previously described methods (Kates et al., 1997; Convit et al., 1999). In short, the amygdala ROIs consisted of three axial slices. The anterior and posterior boundaries were identified at the level of the optic chiasm and the temporal horn of the lateral ventricle, respectively. The superior and inferior-lateral boundaries were identified at the level of the mammalian body and the temporal lobe white matter and extension of the temporal horn, respectively. We also created parametric images of $BP_{ND}$ using the basis function method (Gunn et al., 1997) to conduct voxelwise SPM analysis in addition to ROI analysis.

*Statistical analysis*

*ROI correlation analysis.* Estimates of percentage signal change of fear vs baseline condition were extracted from the amygdala for each participant using the MarsBaR toolbox (Brett et al., 2002). The bilateral amygdala ROIs were defined from the WFU-Pickatlas SPM tool (Maldjian et al., 2003) with the aal atlas (Tzourio-Mazoyer et al., 2002). Correlation between $BP_{ND}$ of [$^{11}$C]SCH23390 and [$^{11}$C]FLB457 in the bilateral amygdala and bilateral amygdala fMRI signal change were calculated using SPSS.

*Confirmatory SPM correlation analysis.* Parametric images of $BP_{ND}$ of [$^{11}$C]SCH23390 and [$^{11}$C]FLB457 were analyzed using SPM2. Exactly the same image preprocessings of normalization and smoothing that were used in fMRI data analysis were applied to parametric images of $BP_{ND}$. To conduct multimodality voxelwise correlation analysis between the BOLD signal and DA receptor binding, we used the biological parametric mapping toolbox for SPM (Casanova et al., 2007). Significant clusters were identified if they reached the extent threshold of $p < 0.05$ corrected for multiple comparisons, with a height threshold of $R > 0.6$ ($p < 0.003$ uncorrected).

## Results

Since the face pictures consisted of Caucasian faces (racial outgroup), even novel neutral faces produced amygdala response in several participants (Hart et al., 2000; Schwartz et al., 2003), leading to a blunted contrast of fear minus neutral. Therefore, we combined neutral and fear conditions and used F&N-B contrast for analyses. Group analysis of F&N-B contrast revealed significant bilateral amygdala responses [right amygdala (26, 0, −26), $t = 4.43$, 93 voxels, left amygdala (−20, −2, −26), $Z = 4.96$, 101

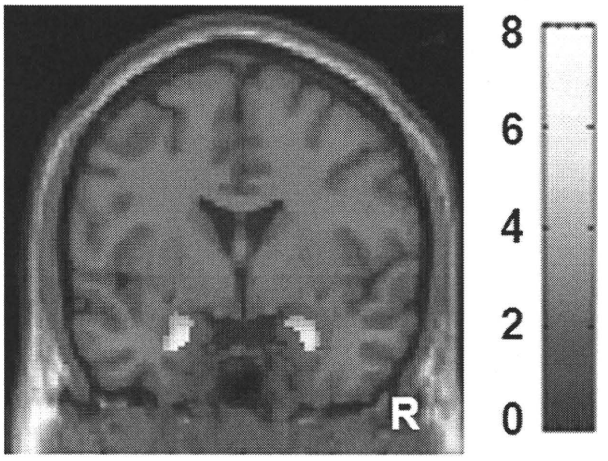


**Figure 1.** Images showing brain response induced by fear and neutral minus baseline condition. Bilateral amygdala responses are shown. The bar shows the range of the *t*-value. R indicates right.

voxels] (Fig. 1). The mean $BP_{ND}$ of [$^{11}$C]SCH23390 in the right and left amygdala were 0.38 ± 0.08 and 0.39 ± 0.11, respectively. The mean $BP_{ND}$ of [$^{11}$C]FLB457 in the right and left amygdala were 2.49 ± 0.50 and 2.50 ± 0.44, respectively.

Correlation analysis of biological parametric mapping revealed that the $BP_{ND}$ value of [$^{11}$C]SCH23390 in the right amygdala was positively correlated with the BOLD signals in the right amygdala of F&N-B contrast [peak (28, 2, −28), 24 voxels] (Fig. 2A). ROIs analysis also revealed a similar significant correlation ($r = 0.59$, $p = 0.005$) in the right amygdala (Fig. 2B), but not in the left amygdala ($r = 0.18$, $p = 0.43$). According to biological parametric mapping analysis, the $BP_{ND}$ value of [$^{11}$C]FLB457 in the amygdala was not correlated with BOLD signals in the amygdala of F&N-B contrast. ROIs analysis showed that right and left amygdala D2 binding was not correlated with the BOLD signals in the right ($r = 0.26$, $p = 0.27$) and left amygdala ($r = 0.28$, $p = 0.23$), respectively. Both biological parametric mapping analysis and ROIs analysis showed that D1 binding in the right and left amygdala was not correlated with D2 binding in the right ($r = 0.24$, $p = 0.30$) and left amygdala ($r = 0.16$, $p = 0.49$), respectively. We used anatomically defined ROIs of the amygdala rather than functional ROIs defined by fMRI in the ROI correlation analysis because it is difficult to place functionally defined ROIs on individual PET data. Anatomically defined ROIs of the amygdala were larger than functionally defined amygdala ROIs. This fact was advantageous in increasing the signal-to-noise ratio in the PET analysis, but led to blunted BOLD signal changes in the amygdala. However, BOLD signal changes derived from both ROI methods were highly correlated with each other. For example, very high correlation ($r = 0.80$, $p < 0.001$) was observed in the right amygdala. Thus, regardless of ROI definition method, we obtained similar results from ROI correlation analyses between BOLD signal changes and DA receptor binding in the amygdala.

## Discussion

Using a multimodality *in vivo* neuroimaging approach, we first directly compared amygdala DA D1 and D2 receptor bindings, indices of receptor availability, with amygdala response evoked by novel or fearful stimuli in human. We found that DA D1 receptors, but not D2 receptors, predicted amygdala response induced by novel facial stimuli with either neutral or fearful expression. Our findings broaden our knowledge about dopaminergic transmission in amygdala response beyond the recent study (Kienast et al., 2008) that elucidated the relation between presynaptic dopamine synthesis and amygdala reactivity.

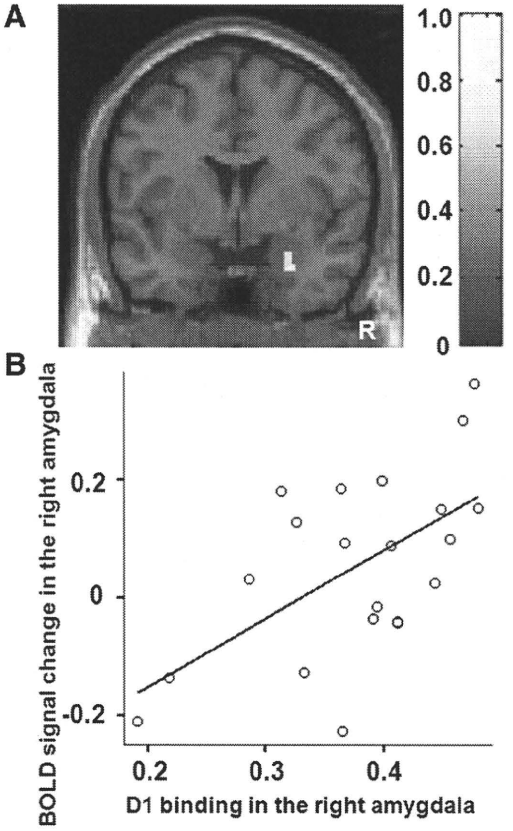


**Figure 2.** ***A***, SPM correlation analysis revealed significant positive linear correlations between D1 binding in the right amygdala and right amygdala signal change. The bar shows the range of the correlation coefficient. ***B***, ROI correlation analysis also revealed similar correlations. R indicates right.

Human neuroimaging studies reported that DA potentiated amygdala response evoked by affective stimuli (Hariri et al., 2002; Tessitore et al., 2002). In rat studies, Rosenkranz and Grace (2002) demonstrated that DA enhances the response of the amygdala by augmenting excitatory sensory input via DA D2 receptor stimulation and attenuating inhibitory prefrontal input to the amygdala through DA D1 receptor stimulation. More recently, it was demonstrated that both D1 and D2 receptor stimulations directly enhanced the excitability of amygdala projection neurons via postsynaptic mechanism (Rosenkranz and Grace, 2002; Kröner et al., 2005; Yamamoto et al., 2007). Amygdala projection neurons are under inhibitory control by GABAergic interneurons (Royer et al., 1999). Both projection neurons and interneurons in the amygdala express DA D1 and D2 receptors (Rosenkranz and Grace, 1999). It has been shown that DA and D1 receptor stimulation augments interneuron excitability and increases the frequency of IPSC in amygdala projection neurons (Kröner et al., 2005). This is a counterintuitive result, considering the fact that DA disinhibits amygdala response *in vivo*. However, Marowsky et al. (2005) found that a subpopulation of amygdala interneurons (paracapsular intercalated cells), located between the major input and output stations of amygdala, is suppressed by DA through D1 receptor stimulation. DA D2 receptors also play a role in disinhibiting amygdala response by decreasing inhibi-

tion onto projection neurons and increasing inhibition onto interneurons (Bissière et al., 2003).

Although detailed examination of subnuclei of the amygdala is difficult in this imaging method, the dorsal portion of the amygdala roughly corresponds to the central nuclei of amygdala (CeA) and the ventral portion of the amygdala corresponds to the basolateral nuclei of amygdala (BLA) and intercalated cell masses (ICM) (Whalen et al., 2009). The amygdala clusters identified both in fMRI task effect analysis and in correlation analysis between D1 binding and amygdala reactivity were located in the ventral portion of the amygdala. Thus, our findings seem to mainly reflect BLA and ICM properties. It is worth mentioning that the highest density of D1 receptors within the amygdala was found in the ICM, followed by BLA, and the expression of D1 receptors is low in CeA (de la Mora et al., 2009; Muly et al., 2009). In contrast, D2 receptors are mainly distributed in CeA (de la Mora et al., 2009). Both D1 and D2 receptors are expressed both postsynaptically in dendrites and presynaptically in axon terminals (Pinto and Sesack, 2008; Muller et al., 2009; Muly et al., 2009), but D1 receptors in BLA are mainly expressed in the dendrites, indicating that DA directly modulates the excitability of BLA projection neurons and interneurons. At the same time, DA also acts on presynaptic D1 receptors to increase the probability of neurotransmitter release from glutamatergic terminals (Muly et al., 2009). Thus, the net DA effect on D1 receptors in the amygdala is a complex mixture of post- and presynaptic actions at several sites.

Although both DA D1 and D2 receptors contribute to potentiating amygdala response via various mechanisms as described above, our finding suggested that DA D1 receptors play a major role in the overall potentiation of amygdala response. At a behavioral level, previous animal studies repeatedly reported that D1 agonist and antagonist applications into the amygdala potentiated and decreased fear response, respectively. However, the effects of D2 agonist/antagonist on fear response have not been well established (Pezze and Feldon, 2004; de la Mora et al., 2009). Thus, the current finding could be regarded as being consistent with previous behavioral pharmacological studies. The combination of PET molecular imaging and fMRI seems to represent a powerful approach for understanding molecular functions in system neuroscience. However, this study has several limitations. First, current PET techniques for human do not have enough spatial resolution to distinguish subnuclei of the amygdala. Although analysis of parametric images of $BP_{ND}$ has become well established (Gunn et al., 1997) and is used in many [$^{11}$C]SCH23390 and [$^{11}$C]FLB457 studies (Cervenka et al., 2006; Takahashi et al., 2008; Karlsson et al., 2009; McNab et al., 2009), a very small region or a single voxel is susceptible to partial volume effect. Thus, it is recommended that parametric image analysis should be used in combination with ROI analysis. At the same time, current results merit further investigation with a higher resolution PET scanner. Second, PET imaging cannot tell us the exact location of DA receptors expressed in projection neurons and interneurons. Future animal studies or *in vitro* studies would complement our findings to determine which D1 receptor-mediated mechanism is most responsible for the overall amygdala response. Third, differences in DA receptor occupancies by endogenous DA might affect BP, leading to different excitabilities of neurons. It is known that BP of [11C]SCH23390 is not sensitive to competitive endogenous dopamine even if massive dopamine is released by amphetamine (Abi-Dargham et al., 1999; Chou et al., 1999). However, it is possible that differences in receptor affinity might contribute to differences in DA receptor occupancies, although Farde et al. (1995) reported that variability in D2 receptor affinity is smaller than that in D2 receptor density. Finally, gender and race effects might also be possible. Any generalization should be approached with caution. Notwithstanding these limitations, we expect our finding to contribute to a broadening of the knowledge of the molecular mechanism of functional abnormalities of the amygdala implicated in neuropsychiatric disorders such as schizophrenia (Takahashi et al., 2004), depression (Drevets, 2000) and Parkinson's disease (Tessitore et al., 2002).

## References


Abi-Dargham A, Simpson N, Kegeles L, Parsey R, Hwang DR, Anjilvel S, Zea-Ponce Y, Lombardo I, Van Heertum R, Mann JJ, Foged C, Halldin C, Laruelle M (1999) PET studies of binding competition between endogenous dopamine and the D1 radiotracer [$^{11}$C] NNC 756. Synapse 32:93–109.

Asan E (1998) The catecholaminergic innervation of the rat amygdala. Adv Anat Embryol Cell Biol 142:1–118.

Bissière S, Humeau Y, Lüthi A (2003) Dopamine gates LTP induction in lateral amygdala by suppressing feedforward inhibition. Nat Neurosci 6:587–592.

Brett M, Anton J, Valabregue R, Poline J (2002) Region of interest analysis using the MarsBar toolbox [abstract]. Paper presented at 8th International Conference on Functional Mapping of the Human Brain, Sendai, Japan.

Casanova R, Srikanth R, Baer A, Laurienti PJ, Burdette JH, Hayasaka S, Flowers L, Wood F, Maldjian JA (2007) Biological parametric mapping: a statistical toolbox for multimodality brain image analysis. Neuroimage 34:137–143.

Cervenka S, Pålhagen SE, Comley RA, Panagiotidis G, Cselényi Z, Matthews JC, Lai RY, Halldin C, Farde L (2006) Support for dopaminergic hypoactivity in restless legs syndrome: a PET study on D2-receptor binding. Brain 129:2017–2028.

Chou YH, Karlsson P, Halldin C, Olsson H, Farde L (1999) A PET study of D1-like dopamine receptor ligand binding. Psychopharmacology 146:220–227.

Convit A, McHugh P, Wolf OT, de Leon MJ, Bobinski M, De Santi S, Roche A, Tsui W (1999) MRI volume of the amygdala: a reliable method allowing separation from the hippocampal formation. Psychiatry Res 90:113–123.

de la Mora MP, Gallegos-Cari A, Arizmendi-Garcia Y, Marcellino D, Fuxe K (2009) Role of dopamine receptor mechanisms in the amygdaloid modulation of fear and anxiety: structural and functional analysis. Prog Neurobiol. Advance online publication. Retrieved October 21, 2009. doi:10.1016/j.pneurobio.2009.10.010.

Drevets WC (2000) Functional anatomical abnormalities in limbic and prefrontal cortical structures in major depression. Prog Brain Res 126:413–431.

Farde L, Halldin C, Stone-Elander S, Sedvall G (1987) PET analysis of human dopamine receptor subtypes using 11C-SCH 23390 and 11C-raclopride. Psychopharmacology (Berl) 92:278–284.

Farde L, Hall H, Pauli S, Halldin C (1995) Variability in D2-dopamine receptor density and affinity: a PET study with [$^{11}$C] raclopride in man. Synapse 20:200–208.

Gunn RN, Lammertsma AA, Hume SP, Cunningham VJ (1997) Parametric imaging of ligand-receptor binding in PET using a simplified reference region model. Neuroimage 6:279–287.

Hariri AR, Mattay VS, Tessitore A, Fera F, Smith WG, Weinberger DR (2002) Dextroamphetamine modulates the response of the human amygdala. Neuropsychopharmacology 27:1036–1040.

Hart AJ, Whalen PJ, Shin LM, McInerney SC, Fischer H, Rauch SL (2000) Differential response in the human amygdala to racial outgroup vs ingroup face stimuli. Neuroreport 11:2351–2355.

Inglis FM, Moghaddam B (1999) Dopaminergic innervation of the amygdala is highly responsive to stress. J Neurochem 72:1088–1094.

Innis RB, Cunningham VJ, Delforge J, Fujita M, Gjedde A, Gunn RN, Holden J, Houle S, Huang SC, Ichise M, Iida H, Ito H, Kimura Y, Koeppe RA, Knudsen GM, Knuuti J, Lammertsma AA, Laruelle M, Logan J, Maguire RP, et al. (2007) Consensus nomenclature for in vivo imaging of reversibly binding radioligands. J Cereb Blood Flow Metab 27:1533–1539.

Ito H, Takahashi H, Arakawa R, Takano H, Suhara T (2008) Normal data-

base of dopaminergic neurotransmission system in human brain measured by positron emission tomography. Neuroimage 39:555–565.

Karlsson S, Nyberg L, Karlsson P, Fischer H, Thilers P, Macdonald S, Brehmer Y, Rieckmann A, Halldin C, Farde L, Bäckman L (2009) Modulation of striatal dopamine D1 binding by cognitive processing. Neuroimage 48:398–404.

Kates W, Abrams M, Kaufmann W, Breiter S, Reiss A (1997) Reliability and validity of MRI measurement of the amygdala and hippocampus in children with fragile X syndrome. Psychiatry Res 75:31–48.

Kienast T, Hariri AR, Schlagenhauf F, Wrase J, Sterzer P, Buchholz HG, Smolka MN, Gründer G, Cumming P, Kumakura Y, Bartenstein P, Dolan RJ, Heinz A (2008) Dopamine in amygdala gates limbic processing of aversive stimuli in humans. Nat Neurosci 11:1381–1382.

Kröner S, Rosenkranz JA, Grace AA, Barrionuevo G (2005) Dopamine modulates excitability of basolateral amygdala neurons in vitro. J Neurophysiol 93:1598–1610.

Lammertsma AA, Hume SP (1996) Simplified reference tissue model for PET receptor studies. Neuroimage 4:153–158.

LeDoux JE (2000) Emotion circuits in the brain. Annu Rev Neurosci 23:155–184.

Lundqvist D, Flykt A, Ohman A (1998) The Karolinska Directed Emotional Faces. Psychology section, Department of Clinical Neuroscience, Karolinska Institute, Stockholm, Sweden.

Maldjian JA, Laurienti PJ, Kraft RA, Burdette JH (2003) An automated method for neuroanatomic and cytoarchitectonic atlas-based interrogation of fMRI data sets. Neuroimage 19:1233–1239.

Marowsky A, Yanagawa Y, Obata K, Vogt KE (2005) A specialized subclass of interneurons mediates dopaminergic facilitation of amygdala function. Neuron 48:1025–1037.

McNab F, Varrone A, Farde L, Jucaite A, Bystritsky P, Forssberg H, Klingberg T (2009) Changes in cortical dopamine D1 receptor binding associated with cognitive training. Science 323:800–802.

Muller JF, Mascagni F, McDonald AJ (2009) Dopaminergic innervation of pyramidal cells in the rat basolateral amygdala. Brain Struct Funct 213:275–288.

Muly EC, Senyuz M, Khan ZU, Guo JD, Hazra R, Rainnie DG (2009) Distribution of D1 and D5 dopamine receptors in the primate and rat basolateral amygdala. Brain Struct Funct 213:375–393.

Olsson H, Halldin C, Swahn CG, Farde L (1999) Quantification of [11C]FLB 457 binding to extrastriatal dopamine receptors in the human brain. J Cereb Blood Flow Metab 19:1164–1173.

Pezze MA, Feldon J (2004) Mesolimbic dopaminergic pathways in fear conditioning. Prog Neurobiol 74:301–320.

Pinto A, Sesack SR (2008) Ultrastructural analysis of prefrontal cortical inputs to the rat amygdala: spatial relationships to presumed dopamine axons and D1 and D2 receptors. Brain Struct Funct 213:159–175.

Rosenkranz JA, Grace AA (1999) Modulation of basolateral amygdala neuronal firing and afferent drive by dopamine receptor activation in vivo. J Neurosci 19:11027–11039.

Rosenkranz JA, Grace AA (2002) Cellular mechanisms of infralimbic and prelimbic prefrontal cortical inhibition and dopaminergic modulation of basolateral amygdala neurons *in vivo*. J Neurosci 22:324–337.

Royer S, Martina M, Paré D (1999) An inhibitory interface gates impulse traffic between the input and output stations of the amygdala. J Neurosci 19:10575–10583.

Schwartz CE, Wright CI, Shin LM, Kagan J, Whalen PJ, McMullin KG, Rauch SL (2003) Differential amygdalar response to novel versus newly familiar neutral faces: a functional MRI probe developed for studying inhibited temperament. Biol Psychiatry 53:854–862.

Scibilia RJ, Lachowicz JE, Kilts CD (1992) Topographic nonoverlapping distribution of D1 and D2 dopamine receptors in the amygdaloid nuclear complex of the rat brain. Synapse 11:146–154.

Suhara T, Sudo Y, Okauchi T, Maeda J, Kawabe K, Suzuki K, Okubo Y, Nakashima Y, Ito H, Tanada S, Halldin C, Farde L (1999) Extrastriatal dopamine D2 receptor density and affinity in the human brain measured by 3D PET. Int J Neuropsychopharmcol 2:73–82.

Takahashi H, Koeda M, Oda K, Matsuda T, Matsushima E, Matsuura M, Asai K, Okubo Y (2004) An fMRI study of differential neural response to affective pictures in schizophrenia. Neuroimage 22:1247–1254.

Takahashi H, Kato M, Takano H, Arakawa R, Okumura M, Otsuka T, Kodaka F, Hayashi M, Okubo Y, Ito H, Suhara T (2008) Differential contributions of prefrontal and hippocampal dopamine D1 and D2 receptors in human cognitive functions. J Neurosci 28:12032–12038.

Tessitore A, Hariri AR, Fera F, Smith WG, Chase TN, Hyde TM, Weinberger DR, Mattay VS (2002) Dopamine modulates the response of the human amygdala: a study in Parkinson's disease. J Neurosci 22:9099–9103.

Tzourio-Mazoyer N, Landeau B, Papathanassiou D, Crivello F, Etard O, Delcroix N, Mazoyer B, Joliot M (2002) Automated anatomical labeling of activations in SPM using a macroscopic anatomical parcellation of the MNI MRI single-subject brain. Neuroimage 15:273–289.

Whalen PJ, Davis C, Oler JA, Kim H, Kim J, Neta M (2009) Human amygdala responses to facial expressions of emotions. In: The human amygdala (Whalen PJ, Phelps EA, eds), pp 265–288. New York: Guilford.

Yamamoto R, Ueta Y, Kato N (2007) Dopamine induces a slow afterdepolarization in lateral amygdala neurons. J Neurophysiol 98:984–992.

Neuroscience Research xxx (2010) xxx–xxx

Contents lists available at ScienceDirect

Neuroscience Research

journal homepage: www.elsevier.com/locate/neures

# Cerebral activation associated with speech sound discrimination during the diotic listening task: An fMRI study

Yumiko Ikeda[a], Noriaki Yahata[a,1], Hidehiko Takahashi[b], Michihiko Koeda[c], Kunihiko Asai[d], Yoshiro Okubo[c], Hidenori Suzuki[a,*]

[a] Department of Pharmacology, Nippon Medical School, 1-1-5, Sendagi, Bunkyo-ku, Tokyo 113-8602, Japan
[b] Department of Molecular Neuroimaging, Molecular Imaging Center, National Institute of Radiological Sciences, 4-9-1, Anagawa, Inage-ku, Chiba 263-8555, Japan
[c] Department of Neuropsychiatry, Nippon Medical School, 1-1-5, Sendagi, Bunkyo-ku, Tokyo 113-8602, Japan
[d] Asai Hospital, 38-1, Katoku, Togane, Chiba 283-0062, Japan

ARTICLE INFO

*Article history:*
Received 22 July 2009
Received in revised form 4 February 2010
Accepted 5 February 2010

*Keywords:*
Auditory attention
Diotic listening
Functional MRI
Left anterior superior temporal gyrus
Left inferior temporal gyrus
Right superior temporal gyrus

ABSTRACT

Comprehending conversation in a crowd requires appropriate orienting and sustainment of auditory attention to and discrimination of the target speaker. While a multitude of cognitive functions such as voice perception and language processing work in concert to subserve this ability, it is still unclear which cognitive components critically determine successful discrimination of speech sounds under constantly changing auditory conditions. To investigate this, we present a functional magnetic resonance imaging (fMRI) study of changes in cerebral activities associated with varying challenge levels of speech discrimination. Subjects participated in a diotic listening paradigm that presented them with two news stories read simultaneously but independently by a target speaker and a distracting speaker of incongruent or congruent sex. We found that the voice of distracter of congruent rather than incongruent sex made the listening more challenging, resulting in enhanced activities mainly in the left temporal and frontal gyri. Further, the activities at the left inferior, left anterior superior and right superior loci in the temporal gyrus were shown to be significantly correlated with accuracy of the discrimination performance. The present results suggest that the subregions of bilateral temporal gyri play a key role in the successful discrimination of speech under constantly changing auditory conditions as encountered in daily life.


## 1. Introduction

Selective listening is an auditory process that enables one to attend to a specific speech of interest among a mixture of parallel conversations. Accomplishment of this ability, commonly known as the cocktail party effect, requires not only appropriate orientation and sustainment of auditory attention but also a multitude of concomitant cognitive processes including sound discrimination, human voice recognition, language processing, and so forth. To reveal the underlying neural mechanisms, the so-called dichotic listening paradigm has long been used as an effective measure in combination with neuroimaging studies (Pugh et al., 1996; Beaman et al., 2007). In this paradigm, two different auditory stimuli are presented simultaneously, but with one of the stimuli delivered to one ear and the second to the other ear (Kimura, 1961; Bryden, 1988). The types of auditory stimuli ranged from simple tones (Jäncke et al., 2003; Petkov et al., 2004) to syllables (Lipschutz et al., 2002), to meaningful words (Grady et al., 1997; Jäncke et al., 2001), and to sentences (Hashimoto et al., 2000). Previous imaging studies based on this paradigm and using positron emission tomography (PET) and functional magnetic resonance imaging (fMRI) have revealed brain regions implicated in selective listening. Robust activity is observed in the bilateral temporal lobes, including the superior temporal gyrus (STG) (Tzourio et al., 1997; Alho et al., 1999; Hugdahl et al., 1999; Zatorre et al., 1999; Hashimoto et al., 2000; Jäncke et al., 2001; van den Noort et al., 2008) during dichotic listening tasks. These areas are well known to be involved in auditory perception (van den Noort et al., 2008). In addition, significant activation is found in the lateral frontal (Hashimoto et al., 2000; Lipschutz et al., 2002; Thomsen et al., 2004) and parietal cortices (Hashimoto et al., 2000; Lipschutz et al., 2002; van den Noort et al., 2008). Mid-ventrolateral (BA 45/47) and mid-dorsolateral areas (BA 9/46) in the lateral frontal cortex are involved in pruning out unwanted information by responding selectively to relevant information (Lipschutz et al., 2002). The parietal cortex, especially the temporoparietal junction extending toward the inferior parietal lobe (IPL), plays a major role in attentional orientation during dichotic listening (Lipschutz et al., 2002). Therefore,

* Corresponding author. Tel.: +81 3 3822 2131; fax: +81 3 5814 1684.
*E-mail address:* hsuzuki@nms.ac.jp (H. Suzuki).
[1] Present address: Department of Neuropsychiatry, Graduate School of Medicine, University of Tokyo, 7-3-1, Hongo, Bunkyo-ku, Tokyo 113-8655, Japan.

0168-0102/$ – see front matter © 2010 Elsevier Ireland Ltd and the Japan Neuroscience Society. All rights reserved.
doi:10.1016/j.neures.2010.02.006

Please cite this article in press as: Ikeda, Y., et al., Cerebral activation associated with speech sound discrimination during the diotic listening task: An fMRI study. Neurosci. Res. (2010), doi:10.1016/j.neures.2010.02.006

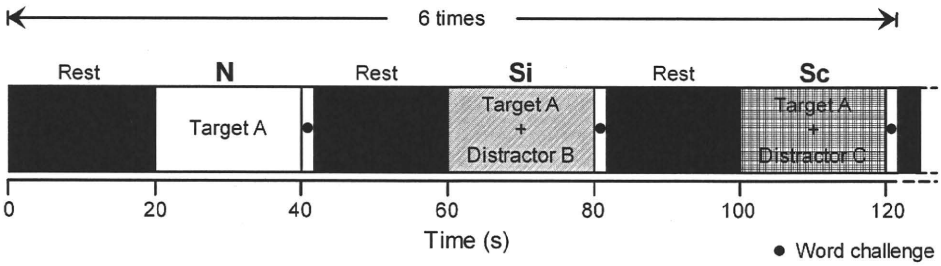


**Fig. 1.** The experimental block design of the session. Three conditions were sequentially presented to subjects: N, non-selective listening, a news story read out by a target speaker only; Si, selective listening, news stories read out by a target speaker and a distracting speaker of incongruent sex; Sc, selective listening, news stories read out by a target speaker and a distracting speaker of congruent sex. Each condition was presented for 20 s and interleaved with 20-s rest. After each condition, a word was displayed on a screen for 2 s (black circle) for the subjects to answer whether or not it was present in the target news of the preceding block by pressing a button. Each session was repeated six times.

the dichotic listening paradigm has a major advantage in specifying brain areas involved in the selective listening process, although speech discrimination under the constantly changing auditory conditions as encountered in daily life is far from such dichotic listening settings.

While the dichotic listening paradigm is one extreme abstraction of selective listening processes that we encounter in daily life, another experimental paradigm, the diotic listening paradigm, has also been used in previous studies, albeit less frequently, to investigate auditory attention under more natural listening settings. The task consists of binaural presentation of target stimuli superimposed by distracting stimuli (Scott et al., 2004; Shafiro and Gygi, 2007), so that the listening condition is more compatible with that in our daily life where the speech of interest and other conversations are typically mixed together and delivered to both ears. Previously, an fMRI study based on this paradigm reported that discrimination of human speech is associated with blood oxygenation level-dependent (BOLD) activation in Wernicke's area (BA22), Broca's area (BA44/45) and the frontal association cortex (BA6, 9/46, 32, 13/47), suggesting that the neural networks for executing semantic, syntactic, and prosodic processing are implicated in speech discrimination (Nakai et al., 2005). Given that constantly changing auditory environments are encountered in daily life, it is still unclear which brain regions critically work in response to change of challenge level in speech sound discrimination paradigms.

Here we present an fMRI study based on the diotic listening paradigm to evaluate brain activity involved in auditory selective attention. We found that hemodynamic activities in some temporal subregions showed significant correlations with performance accuracy of speech sound discrimination.

## 2. Materials and methods

### 2.1. Subjects

Twenty healthy volunteers, 10 males and 10 females, participated in the study (mean age ± SD, 24.9 ± 2.0 years). All subjects were right-handed according to the Edinburgh handedness inventory (mean laterality quotients ± SD, 89.7 ± 15.7) (Oldfield, 1971) and were native speakers of Japanese with normal hearing. None had a previous history of any neurological or psychiatric disorders. All subjects gave written informed consent prior to participation in the experiment. The present study was approved by the Ethics Committees of Nippon Medical School and Asai hospital.

### 2.2. Experimental design

The diotic listening task consisted of three conditions: (1) a reference condition wherein a single news story was read out by a target speaker (N condition), (2) a diotic listening condition wherein two distinct news stories were read out simultaneously but independently by the target and another speaker (distracter) of incongruent sex (Si condition), and (3) the same as Si condition except the sex of the distracter was congruent (Sc condition). Compared to the Si condition, the congruency of the sex of the speaker in the Sc condition was expected to make speech discrimination more challenging, since male and female reportedly have different phonation frequencies in reading possibly due to anatomical differences in vocal folds (Chen, 2007). The expected different levels of difficulty in speech sound discrimination were defined as 'challenge level' hereafter. The news stories were adopted from television programs and segmented into a 20-s long clip by a digital sound editor (Ulead MediaStudio Pro 6.0, Ulead Systems, Torrance, CA, USA). Each news segment contained 2.5 ± 2.3 sentences in each condition, which were read at a rate of 8.6 ± 0.6 characters/s.

A block design was used for the presentation of stimuli during the fMRI session. An active block of 20-s duration, corresponding to one of three listening conditions, was interleaved with resting periods of the same duration (Fig. 1). The order of conditions was fixed to N–Si–Sc, and this sequence was repeated six times in a single session (i.e., six news stories per condition). The target voice remained identical within a single sequence of conditions (N–Si–Sc), so the subjects could identify during the N condition which voice they should have attended to in the subsequent diotic listening conditions (Si and Sc). To avoid habituation to a particular voice, however, the target voices were altered across the sequences.

To quantify the degree of comprehension of stories read by the target voices, a word challenge was employed at each end of the block. A single word was visually presented for 2 s immediately after each block, and the subjects were required to judge if the word was present or absent in the preceding news segment.

The task presentation during the scan was controlled by SuperLab Pro 2.0.4 (Cedrus Corporation, San Pedro, CA, USA). Auditory stimuli were delivered binaurally through headphones (Resonance Technology Inc., Northridge, CA, USA). Visual stimuli were delivered to a translucent mirror attached to a head coil by a projector located outside the scanner room. During the scan, the subjects were instructed to use their index finger when answering the word challenge.

### 2.3. fMRI data acquisition

Functional imaging data were acquired with a 1.5 Tesla Signa system with a standard head coil (General Electric, Milwaukee, WI). Functional images of 180 volumes were acquired from each subject with T2*-weighted gradient-echo echo-planar imaging sequences sensitive to BOLD contrast. Each volume consisted of 40 transaxial contiguous sections with a section thickness of 3 mm to cover almost the whole brain (flip angle, 90°; TE, 50 ms; TR, 4 s; matrix, 64 × 64; field of view, 24 cm × 24 cm).

### 2.4. fMRI data analysis

Data analysis was performed with statistical parametric mapping software 2 (SPM2; Wellcome Department of Cognitive Neurology, University College London, UK) running with MATLAB (Mathworks, Natick, MA). All volumes were realigned to the first volume in each session to correct for head motion and were then spatially normalized to the standard space defined by the Montreal Neurological Institute template. After normalization, all scans had a resolution of 3 mm × 3 mm × 3 mm. Functional images were spatially smoothed with a 3D isotropic Gaussian kernel (full width at half maximum of 8 mm). Low frequency noise was removed by applying a high-pass filter (cutoff period, 80 s) to the fMRI time-series data of each voxel. For subject-level statistical analyses, significant hemodynamic changes in each condition (N, Si, Sc) were examined using the general linear model with boxcar functions convolved with a hemodynamic response function. Statistical parametric maps for each contrast (Si–N, Sc–N, Sc–Si) of the *t*-statistic were calculated on a voxel-by-voxel basis.

For group comparisons, random effect analyses were performed. The contrast images obtained from subject-level statistical analyses were entered into the random effects analyses. One-sample *t*-test was performed to determine group activation for each effect. A height threshold of $P < 0.001$ (uncorrected) and an extent threshold of 10 voxels were considered significant. For anatomical localization, peak voxels were converted from MNI to Talairach coordinates (Talairach and Tournoux, 1988).

Please cite this article in press as: Ikeda, Y., et al., Cerebral activation associated with speech sound discrimination during the diotic listening task: An fMRI study. Neurosci. Res. (2010), doi:10.1016/j.neures.2010.02.006

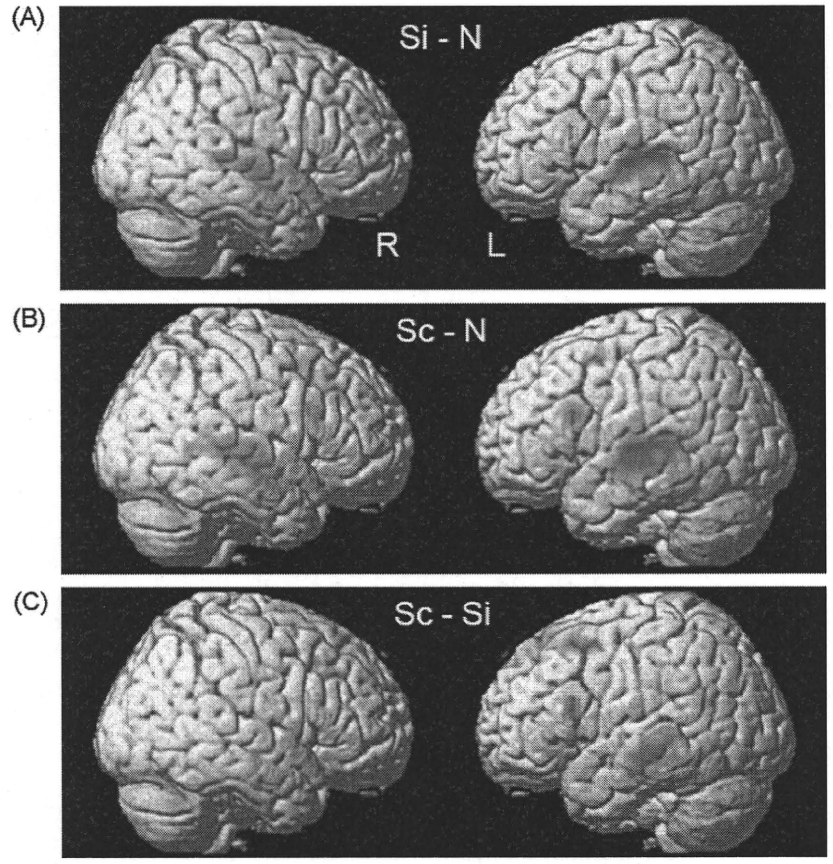


**Fig. 2.** Cortical rendering of activated areas in selective listening task. (A) Activation in the Si–N constrast. The bilateral temporal, frontal and parietal areas were activated. (B) Activation in the Sc–N contrast. The bilateral temporal, frontal areas, the left insula, cerebellum and the right parietal areas were activated. Compared with Si–N contrast, wider areas were activated in Sc–N contrast. (C) Activation in the Sc–Si contrast. The bilateral temporal, frontal areas and the left parietal areas were activated. All images are shown at the height threshold of $P = 0.001$, uncorrected, and the extent threshold of $k = 10$ voxels.

### 2.5. Performance analysis of word challenge

Performance score of the word challenge was obtained by counting the number of words that the subjects could answer correctly in the individual conditions with six repetitions. The accuracy rate was expressed as percent of the total number of correct words against all six sequences, and the values were shown as mean ± SD. The accuracy rate was compared among N, Si and Sc conditions using one-way ANOVA, followed by Tukey's multiple comparison test. $P < 0.05$ was considered statistically significant.

Simple regression analyses were performed to examine correlations between task-related BOLD signal changes of Sc–Si contrast and the performance score difference between Si and Sc conditions (Sc–Si). Pearson's correlation coefficient was then calculated with a significance threshold of $P < 0.05$.

## 3. Results

### 3.1. fMRI data

To assess the areas activated in selective listening attention under this designed experiment, the BOLD signal changes in both Si–N and Sc–N contrasts were examined. In Si–N contrast, as shown in Fig. 2A, the bilateral STG, middle temporal gyrus (MTG), middle frontal gyrus (MFG), superior parietal lobule (SPL), left precentral gyrus, right inferior frontal gyrus (IFG), precuneus and IPL were significantly activated (Table 1 and Fig. 2A). In Sc–N contrast, there was significant activation in the bilateral STG, MTG, IFG and MFG, the left insula and cerebellum, right medial frontal gyrus, precuneus, supramarginal gyrus (SMG) and inferior parietal gyrus (Table 1 and Fig. 2B). These results suggest that the brain regions activated in Sc condition are more widespread than those in Si condition.

Furthermore, the difference in BOLD signal between Sc and Si conditions was analyzed to reveal how the change of challenge level in speech sound discrimination affects brain hemodynamic activity. In Sc–Si contrast, significant activations were observed in the bilateral STG, MTG, IFG, MFG, medial frontal gyrus, SFG, left inferior temporal gyrus (ITG), SMG and IPL (Table 1 and Fig. 2C).

### 3.2. Accuracy rate

Next, we investigated whether the difference in challenge level in speech sound discrimination among three conditions reflects the difference in accuracy rate. The subjects judged the presence of the keywords in the preceding narration with 93.3 ± 8.4% (N condition), 92.5 ± 10.1% (Si), and 81.7 ± 17.1% (Sc) of accuracy rates, respectively (ANOVA for group comparison, $P = 0.0065$; Fig. 3). Thus, the subjects answered the target word less correctly in Sc condition than in N and Si conditions ($P < 0.05$), suggesting that they had more difficulty in discriminating the target voice when the distracter was of congruent sex in Sc condition.

### 3.3. Correlation between fMRI image and performance score

Further, we sought to determine the brain regions responsible for changes of challenge level in speech sound discrimination as measured by BOLD activation. The change in BOLD signal under Sc–Si contrast was positively correlated with the difference in performance score between Si and Sc conditions (Sc–Si) in the left ITG (BA 20, $R = 0.796$, $P < 0.001$), left anterior STG (BA 38, $R = 0.787$,

Please cite this article in press as: Ikeda, Y., et al., Cerebral activation associated with speech sound discrimination during the diotic listening task: An fMRI study. Neurosci. Res. (2010), doi:10.1016/j.neures.2010.02.006

**Table 1**
Regions activated in selective listening in Si–N, Sc–N and Sc–Si contrasts.

| Contrast | Hemisphere | Region (Brodmann area) | Talairach | | | *t*-Value |
|---|---|---|---|---|---|---|
| | | | *x* | *y* | *z* | |
| Si–N | L | Superior temporal gyrus (22) | −59 | −25 | 7 | 10.59 |
| | | Middle temporal gyrus (21) | −59 | −6 | −5 | 6.24 |
| | | Precentral gyrus (6/4) | −57 | 7 | 31 | 6.92 |
| | | Middle frontal gyrus (46) | −48 | 42 | 20 | 4.13 |
| | | Superior parietal lobule (7) | −12 | −65 | 55 | 4.33 |
| | R | Superior temporal gyrus (22/42) | 61 | −33 | 7 | 5.88 |
| | | Middle temporal gyrus (21) | 67 | −14 | −4 | 5.73 |
| | | Middle frontal gyrus (10/9/46) | 36 | 47 | 11 | 4.67 |
| | | Inferior frontal gyrus (44) | 53 | 13 | 21 | 4.34 |
| | | Superior parietal lobule (7) | 18 | −69 | 50 | 6.65 |
| | | Precuneus (7) | 16 | −54 | 52 | 4.36 |
| | | Inferior parietal lobule (40) | 57 | −42 | 22 | 4.04 |
| Sc–N | L | Superior temporal gyrus (22/42) | −51 | −17 | 3 | 12.08 |
| | | Middle temporal gyrus (21) | −53 | −12 | −6 | 10.28 |
| | | Inferior frontal gyrus (45) | −57 | 20 | 19 | 8.01 |
| | | Middle frontal gyrus (6) | −46 | 4 | 50 | 6.24 |
| | | Insula | −30 | 19 | −1 | 4.82 |
| | | Cerebellum | −14 | −79 | −21 | 5.39 |
| | R | Middle temporal gyrus (21) | 61 | −6 | −11 | 7.85 |
| | | Superior temporal gyrus (22/42) | 63 | −29 | 5 | 6.06 |
| | | Inferior frontal gyrus (45/44/47) | 59 | 19 | 21 | 6.37 |
| | | Middle frontal gyrus (6/10/9/8/46) | 48 | 8 | 46 | 5.09 |
| | | Medial frontal gyrus (8) | 2 | 37 | 41 | 4.18 |
| | | Precuneus (7) | 14 | −62 | 40 | 4.85 |
| | | Supramarginal gyrus (40) | 44 | −43 | 37 | 4.67 |
| | | Inferior parietal lobule (39) | 48 | −58 | 43 | 4.45 |
| Sc–Si | L | Middle temporal gyrus (21) | −55 | −20 | −7 | 6.66 |
| | | Superior temporal gyrus (22/38) | −46 | −23 | 3 | 5.7 |
| | | Inferior temporal gyrus (20) | −46 | −7 | −25 | 4.47 |
| | | Inferior frontal gyrus (45/47) | −53 | 18 | 14 | 6.5 |
| | | Middle frontal gyrus (8/6) | −32 | 22 | 47 | 6.35 |
| | | Medial frontal gyrus (8) | −2 | 31 | 46 | 6.21 |
| | | Superior frontal gyrus (8/6) | −8 | 34 | 52 | 5.37 |
| | | Supramarginal gyrus (40) | −63 | −47 | 28 | 5.56 |
| | | Inferior parietal lobule (39/40) | −50 | −59 | 23 | 5.02 |
| | R | Middle temporal gyrus (21) | 53 | 1 | −25 | 4.92 |
| | | Superior temporal gyrus (22) | 46 | −21 | 3 | 4.6 |
| | | Medial frontal gyrus (8/9) | 2 | 39 | 40 | 5.08 |
| | | Superior frontal gyrus (8) | 8 | 50 | 36 | 4.84 |
| | | Inferior frontal gyrus (45) | 8 | 36 | 52 | 4.75 |
| | | Middle frontal gyrus (8/9/6/46) | 61 | 22 | 21 | 4.44 |

$P<0.001$) and right STG (BA 22, $R=0.722$, $P<0.001$), respectively (Table 2 and Fig. 4). The two subregions in the left temporal gyrus (BA 20 and 38) were also included in activated areas under Sc–Si contrast by the overall analysis as shown in Table 1 (superior temporal gyrus and inferior temporal gyrus). At the individual level, 10 subjects showed no difference in the performance score between Sc and Si conditions, while they had increase in BOLD signal in the left ITG and left anterior STG under Sc–Si contrast (Fig. 4A and B). As for the right STG BOLD signal, seven subjects with lower performance score showed lower BOLD activity in this subregion under Sc condition than Si condition (Fig. 4C).

**Table 2**
Regions of activation correlated with performance score in Sc–Si contrast.

| Hemisphere | Region (Brodmann area) | Talairach | | | *t*-Value |
|---|---|---|---|---|---|
| | | *x* | *y* | *z* | |
| L | Inferior temporal gyrus (20) | −50 | −32 | −10 | 5.31 |
| | Superior temporal gyrus (38) | −48 | 12 | −28 | 4.46 |
| R | Superior temporal gyrus (22) | 63 | −8 | 0 | 4.66 |

## 4. Discussion

### 4.1. Cortical network in auditory selective attention

By means of fMRI with a diotic experimental paradigm based rather on actual human conversation, cortical hemodynamic response was observed robustly in the bilateral STG and MTG and substantially in the bilateral MFG, right IFG and SPL in both Si and Sc conditions. Brain imaging (PET and fMRI) combined with dichotic listening task (O'Leary et al., 1996; Hugdahl et al., 1999, 2000; Hashimoto et al., 2000; Jäncke et al., 2001, 2003; Hund-Georgiadis et al., 2002) has already been extensively used to reveal the regions responsible for attentive listening. These studies have demonstrated widespread activities not only in the temporal cortex including bilateral STG and MTG, but also in the inferior parietal and prefrontal cortices (Jäncke and Shah, 2002; Lipschutz et al., 2002). In addition, an fMRI study (Nakai et al., 2005) using a diotic listening paradigm has also shown similar brain activation in the frontal association cortex as well as STG. Therefore, brain regions activated during the present diotic listening task are consistent with those previously reported, suggesting that the present task mimicking daily life conditions can efficiently activate the auditory attention networks commonly used during selective listening.

Please cite this article in press as: Ikeda, Y., et al., Cerebral activation associated with speech sound discrimination during the diotic listening task: An fMRI study. Neurosci. Res. (2010), doi:10.1016/j.neures.2010.02.006

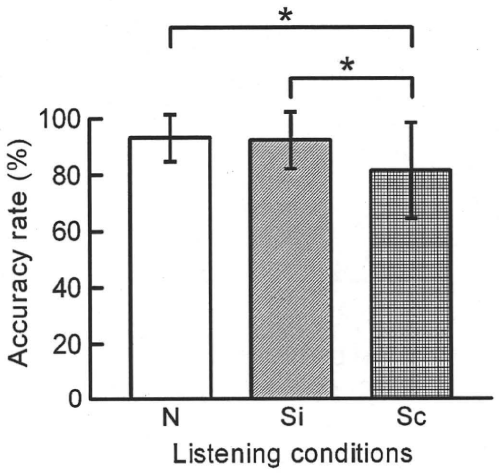


**Fig. 3.** Accuracy rate of word challenge. The ratio (%) of the number of target words correctly answered by the subjects in the individual conditions in the session was calculated and referred to as accuracy rate. The values were mean ± SD. The accuracy rates were significantly different among the three conditions ($F(2, 57) = 5.5$, $P = 0.0065$). Sc condition has significantly lower accuracy rate compared with N and Si conditions (*$P < 0.05$). N, non-selective listening; Si, selective listening with speakers of incongruent sex; Sc, selective listening with speakers of congruent sex. $n = 20$.

### 4.2. Diotic selective listening

To accomplish the diotic listening task in the present study, several distinct steps were required to process auditory information: discriminating the voice of the target speaker from that of the distracter, ignoring the distracter's voice, keeping attention focused on the story read by the target speaker, recognizing the words in the story, constructing sentences from the words, and comprehending and memorizing the sentences. In each process, distinct brain regions are thought to be involved. The right anterior part of the superior temporal sulcus and right IFG are reportedly involved in the prosodic component of speech sound processing (Plante et al., 2002; Zatorre et al., 2002) to discriminate the target voice by comparing it with others' prosodic features. The left frontal (BA 6, 8, 9, 44 and 46) and parietal lobes (BA7) have been thought to have a role in ignoring distracter stimuli (Bledowski et al., 2004). Broca's area (BA 44 and 45) is involved in syntactic processing (Stromswold et al., 1996; Caplan et al., 1999). It has been reported that the anterior areas of the left superior temporal gyrus and middle temporal gyrus are involved in speech comprehension (Scott et al., 2000; Davis and Johnsrude, 2003) and the left parietal cortex in working memory retrieval or short-time memory (Majerus et al., 2007; Öztekin et al., 2009). As shown by the results, the present task increased hemodynamic activation in the above-mentioned areas, consistent with the previous observations. Collectively, the present results suggest that the temporal, parietal and frontal regions are extensively involved in overall information processing during selective diotic listening.

However, there are several differences in the activated area between the previous dichotic listening studies and the present results. Activation of the primary auditory area such as BA 41 was not significant at the statistical threshold applied in the present study, while previous dichotic listening task studies found predominant activation in the primary auditory cortex contralateral to the ear of stimulation (Alho et al., 1999; Jäncke et al., 2001). Most of the auditory stimuli adopted in previous dichotic listening task studies were tone and syllables, whereas in the present task we used as stimuli two different contents of sentences read simultaneously but independently by a target and a distracting speaker. Under such condition, the subjects are required to execute neural processes pertaining to lexical access and semantic retrieval for completion of the task. Therefore, the cerebral activation might rather reflect post-sensory linguistic processing. In fact, functional neuroimaging studies using speech as stimuli showed activation of the left-lateralized networks, including the parietal, frontal and temporal cortex (Binder et al., 2009).

In addition, our results showed activation in the bilateral parietal cortices (BA 7) in Si–N contrast, the right parietal cortex (BA 39) in Sc–N contrast, and the left parietal cortex (BA 39 and 40) in Sc–Si contrast. While dichotic listening tasks have been reported to preferentially activate the right parietal cortex in association with spatial auditory processing (Alho and Vorobyev, 2007), left-dominant brain activation has been reported in angular gyrus (BA 39) and its adjacent areas (BA 40 and 7) in the semantic decision task using spoken languages (Binder et al., 1997, 2009). Accordingly, the parietal cortex activation shown in our task may be due to language processing rather than spatial processing.

### 4.3. Change of challenge level in speech sound discrimination and hemodynamic response in fMRI

As expected from the sex difference in voice properties, Sc condition was more difficult for the subjects to discriminate speech than Si condition when the mean accuracy rate in the performance was compared between Sc and Si conditions. Furthermore, the difference in performance between Si and Sc conditions was positively correlated with the change in BOLD signal under Sc–Si contrast in the left ITG, left anterior and right STG. At the individual level, half of the subjects showed increase in BOLD signal in the left ITG and left anterior STG without apparent difference in performance score between Sc and Si conditions. These results might be interpreted as the subjects making effort to attain good performance, resulting in BOLD increase in these regions. As described above, it has been reported that the left ITG and left anterior STG are involved in lexical–semantic processing (Binder et al., 2009). On the other hand, seven subjects with lower performance score under Sc condition than Si condition showed lower BOLD activity in the right STG. This implies that the activity of this subregion, which reportedly involves sentential prosody processing (Plante et al., 2002; Zatorre et al., 2002), may directly reflect the ability to discriminate performance. The involvement of these regions in successful discrimination may, therefore, indicate that the our present tasks require linguistic processing in addition to phonological one; since targeted words were presented in the news articles, the participants need to comprehend the target speech in the context of the news contents as well as to differentiate the target voice in the context of the phonetic feature. Collectively, these results suggest that these temporal subregions relating to language processing also play important roles in performing speech discrimination under constantly changing auditory conditions intermingled with different speakers' voices.

### 4.4. Selective auditory attention and psychiatric disorders

Patients with psychiatric disorders are known to often suffer from attention disturbance. For instance, deficit in attention has been thought to be a primary feature of neurocognitive profiles of patients with schizophrenia on the basis of neuropsychological studies (Heinrichs and Zakzanis, 1998; Fioravanti et al., 2005). Intriguingly, functional imaging studies of attention and working memory, however, have reported mixed findings in these patients. Attention task-related activation is attenuated in schizophrenia in DLPFC (Ojeda et al., 2002) and STG (Gallinat et al., 2002) as compared to in healthy subjects. In contrast, enhanced activa-

Please cite this article in press as: Ikeda, Y., et al., Cerebral activation associated with speech sound discrimination during the diotic listening task: An fMRI study. Neurosci. Res. (2010), doi:10.1016/j.neures.2010.02.006

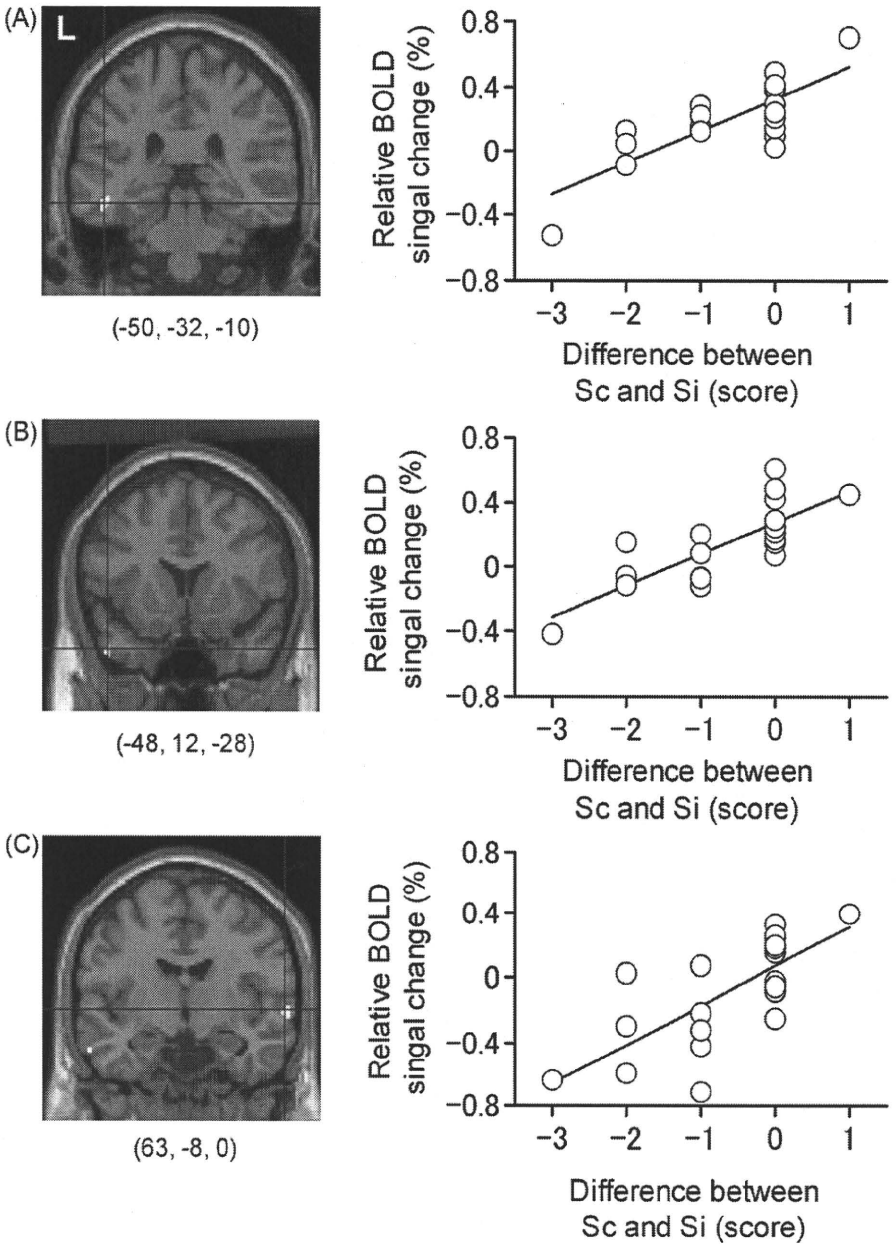


**Fig. 4.** Correlation between relative BOLD signal change and performance score difference in Sc–Si contrast. In the right panels, the vertical axes represent relative BOLD signal change in Sc–Si contrast, and the horizontal axes indicate the difference in performance score between Si and Sc conditions. Scatter plots illustrate significant positive correlations by simple regression analyses between neural activation of the left inferior temporal gyrus (A), left anterior superior temporal gyrus (B), or right superior temporal gyrus (C) and the performance score difference (Sc–Si). The left panels illustrate the brain regions with corresponding Talairach coordinates showing the correlations as described.

tion in DLPFC (Weiss et al., 2003) and STG (Weiss et al., 2007; Schirmer et al., 2009) has been observed in schizophrenia. Such discrepancy may be derived not only from the wide variety of patient profiles, but also task designs, which focus on different aspects of neurocognitive function of patients. A key feature of the paradigm used in the present study is that it could uniquely depict the brain activity during listening attention encountered in the daily conversational environment. In addition, this task can measure an activity change of the speech sound discrimination in temporal areas, which is reportedly reduced in volume in patients with schizophrenia (Collinson et al., 2009; Sun et al., 2009). Therefore, future studies using the present diotic task may be useful for investigating the cognitive aspect of auditory attention in patients with attention disturbance such as schizophrenia.

**Acknowledgments**

We thank the staffs of Asai hospital for their assistance in collecting the demographic data. Funding for this study was provided by a Grant-in-Aid for Science Research (C) from the Ministry of Education, Culture, Sports, Science, and Technology (MEXT), Japan, to H.S. (no. 1659028), a Grant-in-Aid for Encouragement of Young Scientists (B) from the Japan Society for the Promotion of Science (JSPS) to N.Y. (no. 18790852) and to Y.I. (no. 17790821).

**References**

Alho, K., Medvedev, S.V., Pakhomov, S.V., Roudas, M.S., Tervaniemi, M., Reinikainen, K., Zeffiro, T., Näätänen, R., 1999. Selective tuning of the left and right auditory cortices during spatially directed attention. Cogn. Brain Res. 7, 335–341.

Please cite this article in press as: Ikeda, Y., et al., Cerebral activation associated with speech sound discrimination during the diotic listening task: An fMRI study. Neurosci. Res. (2010), doi:10.1016/j.neures.2010.02.006

Alho, K., Vorobyev, V.A., 2007. Brain activity during selective listening to natural speech. Front. Biosci. 12, 3167–3176.
Beaman, C.P., Bridges, A.M., Scott, S.K., 2007. From dichotic listening to the irrelevant sound effect: a behavioural and neuroimaging analysis of the processing of unattended speech. Cortex 43, 124–134.
Binder, J.R., Frost, J.A., Hammeke, T.A., Cox, R.W., Rao, S.M., Prieto, T., 1997. Human brain language areas identified by functional magnetic resonance imaging. J. Neurosci. 17, 353–362.
Binder, J.R., Desai, R.H., Graves, W.W., Conant, L.L., 2009. Where is the semantic system? A critical review and meta-analysis of 120 functional neuroimaging studies. Cereb. Cortex 19, 2767–2796.
Bledowski, C., Prvulovic, D., Goebel, R., Zanella, F.E., Linden, D.E.J., 2004. Attentional systems in target and distractor processing: a combined ERP and fMRI study. Neuroimage 22, 530–540.
Bryden, M.P., 1988. Correlates of the dichotic right-ear effect. Cortex 24, 313–319.
Caplan, D., Alpert, N., Waters, G., 1999. PET studies of syntactic processing with auditory sentence presentation. Neuroimage 9, 343–351.
Chen, S.H., 2007. Sex differences in frequency and intensity in reading and voice range profiles for Taiwanese adult speakers. Folia Phoniatr. Logop. 59, 1–9.
Collinson, S.L., Mackay, C.E., Jiaqing, O., James, A.C.D., Crow, T.J., 2009. Dichotic listening impairments in early onset schizophrenia are associated with reduced left temporal lobe volume. Schizophr. Res. 112, 24–31.
Davis, M.H., Johnsrude, I.S., 2003. Hierarchical processing in spoken language comprehension. J. Neurosci. 23, 3423–3431.
Fioravanti, M., Carlone, O., Vitale, B., Cinti, M.E., Clare, L., 2005. A meta-analysis of cognitive deficits in adults with a diagnosis of schizophrenia. Neuropsychol. Rev. 15, 73–95.
Gallinat, J., Mulert, C., Bajbouj, M., Herrmann, W.M., Schunter, J., Senkowski, D., Moukhtieva, R., Kronfeldt, D., Winterer, G., 2002. Frontal and temporal dysfunction of auditory stimulus processing in schizophrenia. Neuroimage 17, 110–127.
Grady, C.L., Van Meter, J.W., Maisog, J.M., Pietrini, P., Krasuski, J., Rauschecker, J.P., 1997. Attention-related modulation of activity in primary and secondary auditory cortex. Neuroreport 8, 2511–2516.
Hashimoto, R., Homae, F., Nakajima, K., Miyashita, Y., Sakai, K.L., 2000. Functional differentiation in the human auditory and language areas revealed by a dichotic listening task. Neuroimage 12, 147–158.
Heinrichs, R.W., Zakzanis, K.K., 1998. Neurocognitive deficit in schizophrenia: a quantitative review of the evidence. Neuropsychology 12, 426–445.
Hugdahl, K., Brønnick, K., Kyllingsbæk, S., Law, I., Gade, A., Paulson, O.B., 1999. Brain activation during dichotic presentations of consonant–vowel and musical instrument stimuli: a $^{15}$O-PET study. Neuropsychologia 37, 431–440.
Hugdahl, K., Law, I., Kyllingsbæk, S., Brønnick, K., Gade, A., Paulson, O.B., 2000. Effects of attention on dichotic listening: an $^{15}$O-PET study. Hum. Brain Mapp. 10, 87–97.
Hund-Georgiadis, M., Lex, U., Friederici, A.D., von Cramon, D.Y., 2002. Non-invasive regime for language lateralization in right- and left-handers by means of functional MRI and dichotic listening. Exp. Brain Res. 145, 166–176.
Jäncke, L., Buchanan, T.W., Lutz, K., Shah, N.J., 2001. Focused and nonfocused attention in verbal and emotional dichotic listening: an FMRI study. Brain Lang. 78, 349–363.
Jäncke, L., Shah, N.J., 2002. Does dichotic listening probe temporal lobe functions? Neurology 58, 736–743.
Jäncke, L., Specht, K., Shah, J.N., Hugdahl, K., 2003. Focused attention in a simple dichotic listening task: an fMRI experiment. Cogn. Brain Res. 16, 257–266.
Kimura, D., 1961. Cerebral dominance and the perception of verbal stimuli. Can. J. Psychol. 15, 166–171.
Lipschutz, B., Kolinsky, R., Damhaut, P., Wikler, D., Goldman, S., 2002. Attention-dependent changes of activation and connectivity in dichotic listening. Neuroimage 17, 643–656.
Majerus, S., Bastin, C., Poncelet, M., Van der Linden, M., Salmon, E., Collette, F., Maquet, P., 2007. Short-term memory and the left intraparietal sulcus: focus of attention? Further evidence from a face short-term memory paradigm. Neuroimage 35, 353–367.
Nakai, T., Kato, C., Matsuo, K., 2005. An fMRI study to investigate auditory attention: a model of the cocktail party phenomenon. Magn. Reson. Med. Sci. 4, 75–82.
Ojeda, N., Ortuño, F., Arbizu, J., López, P., Martí-Climent, J.M., Peñuelas, I., Cervera-Enguix, S., 2002. Functional neuroanatomy of sustained attention in schizophrenia: contribution of parietal cortices. Hum. Brain Mapp. 17, 116–130.
O'Leary, D.S., Andreasen, N.C., Hurtig, R.R., Hichwa, R.D., Watkins, G.L., Ponto, L.L.B., Rogers, M., Kirchner, P.T., 1996. A positron emission tomography study of binaurally and dichotically presented stimuli: effects of level of language and directed attention. Brain Lang. 53, 20–39.
Oldfield, R.C., 1971. The assessment and analysis of handedness: the Edinburgh inventory. Neuropsychologia 9, 97–113.
Öztekin, I., McElree, B., Staresina, B.P., Davachi, L., 2009. Working memory retrieval: contributions of the left prefrontal cortex, the left posterior parietal cortex, and the hippocampus. J. Cogn. Neurosci. 21, 581–593.
Petkov, C.I., Kang, X., Alho, K., Bertrand, O., Yund, E.W., Woods, D.L., 2004. Attentional modulation of human auditory cortex. Nat. Neurosci. 7, 658–663.
Plante, E., Creusere, M., Sabin, C., 2002. Dissociating sentential prosody from sentence processing: activation interacts with task demands. Neuroimage 17, 401–410.
Pugh, K.R., Shaywitz, B.A., Shaywitz, S.E., Fulbright, R.K., Byrd, D., Skudlarski, P., Shankweiler, D.P., Katz, L., Constable, R.T., Fletcher, J., Lacadie, C., Marchione, K., Gore, J.C., 1996. Auditory selective attention: an fMRI investigation. Neuroimage 4, 159–173.
Schirmer, T.N., Dorflinger, J.M., Marlow-O'Connor, M., Pendergrass, J.C., Hartzell, A., All, S.D., Charles, D., 2009. FMRI indices of auditory attention in schizophrenia. Prog. Neuropsychopharmacol. Biol. Psychiatry 33, 25–32.
Scott, S.K., Blank, C.C., Rosen, S., Wise, R.J.S., 2000. Identification of a pathway for intelligible speech in the left temporal lobe. Brain 123, 2400–2406.
Scott, S.K., Rosen, S., Wichham, L., Wise, R.J.S., 2004. A positron emission tomography study of the neural basis of informational and energetic masking effects in speech perception. J. Acoust. Soc. Am. 115, 813–821.
Shafiro, V., Gygi, B., 2007. Perceiving the speech of multiple concurrent talkers in a combined divided and selective attention task. J. Acoust. Soc. Am. 122, EL229–EL235.
Stromswold, K., Caplan, D., Alpert, N., Rauch, S., 1996. Localization of syntactic comprehension by positron emission tomography. Brain Lang. 52, 452–473.
Sun, J., Maller, J.J., Guo, L., Fitzgerald, P.B., 2009. Superior temporal gyrus volume change in schizophrenia: a review on region of interest volumetric studies. Brain Res. Rev. 61, 14–32.
Talairach, J., Tournoux, P., 1988. Co-planar Stereotaxic Atlas of the Human Brain: 3-Dimensional Proportional System—An Approach to Cerebral Imaging. Thieme Medical Publishers, New York.
Thomsen, T., Rimol, L.M., Ersland, L., Hugdahl, K., 2004. Dichotic listening reveals functional specificity in prefrontal cortex: an fMRI study. Neuroimage 21, 211–218.
Tzourio, N., Massioui, F.E., Crivello, F., Joliot, M., Renault, B., Mazoyer, B., 1997. Functional anatomy of human auditory attention studied with PET. Neuroimage 5, 63–77.
van den Noort, M., Specht, K., Rimol, L.M., Ersland, L., Hugdahl, K., 2008. A new verbal reports fMRI dichotic listening paradigm for studies of hemispheric asymmetry. Neuroimage 40, 902–911.
Weiss, E.M., Golaszewski, S., Mottaghy, F.M., Hofer, A., Hausmann, A., Kemmler, G., Kremser, C., Brinkhoff, C., Felber, S.R., Fleischhacker, W.W., 2003. Brain activation patterns during a selective attention test—a functional MRI study in healthy volunteers and patients with schizophrenia. Psychiatry Res. Neuroimaging 123, 1–15.
Weiss, E.M., Siedentopf, C., Golaszewski, S., Mottaghy, F.M., Hofer, A., Kremser, C., Felber, S., Fleischhacker, W.W., 2007. Brain activation patterns during a selective attention test—a functional MRI study in healthy volunteers and unmedicated patients during an acute episode of schizophrenia. Psychiatry Res. Neuroimaging 154, 31–40.
Zatorre, R.J., Mondor, T.A., Evans, A.C., 1999. Auditory attention to space and frequency activates similar cerebral systems. Neuroimage 10, 544–554.
Zatorre, R.J., Belin, P., Penhune, V.B., 2002. Structure and function of auditory cortex: music and speech. Trends Cogn. Sci. 6, 37–46.

Please cite this article in press as: Ikeda, Y., et al., Cerebral activation associated with speech sound discrimination during the diotic listening task: An fMRI study. Neurosci. Res. (2010), doi:10.1016/j.neures.2010.02.006

*International Journal of Neuropsychopharmacology*, Page 1 of 8. Copyright © CINP 2010
doi:10.1017/S1461145710000313

ARTICLE

CINP

# Peripheral benzodiazepine receptors in patients with chronic schizophrenia: a PET study with [$^{11}$C]DAA1106

**Akihiro Takano[1], Ryosuke Arakawa[1], Hiroshi Ito[1], Amane Tateno[2], Hidehiko Takahashi[1], Ryohei Matsumoto[1], Yoshiro Okubo[2] and Tetsuya Suhara[1]**

[1] *Molecular Neuroimaging Group, Molecular Imaging Center, National Institute of Radiological Sciences, Chiba, Japan*
[2] *Department of Neuropsychiatry, Nippon Medical School, Tokyo, Japan*

**Abstract**

Inflammatory/immunological process and glial contribution are suggested in the pathophysiology of schizophrenia. We investigated peripheral benzodiazepine receptors in brains of patients with chronic schizophrenia, which were reported to be located on mitochondria of glial cells, using [$^{11}$C]DAA1106 with positron emission tomography. Fourteen patients and 14 age- and sex-matched normal controls participated in this study. PET data were analysed by two-tissue compartment model with metabolite-corrected plasma input. Clinical symptoms were assessed using the Positive and Negative Syndrome Scale. There was no significant difference between [$^{11}$C]DAA1106 binding of the cortical regions of normal controls and patients with schizophrenia, whereas the patients showed a positive correlation between cortical [$^{11}$C]DAA1106 binding and positive symptom scores. There was also a positive correlation between [$^{11}$C]DAA1106 binding and duration of illness. Although the correlations need to be interpreted very cautiously, involvement of glial reaction process in the pathophysiology of positive symptoms or progressive change of schizophrenia might be suggested.

*Received 18 November 2009; Reviewed 14 December 2009; Revised 29 January 2010; Accepted 27 February 2010*

**Key words**: Microglia, peripheral benzodiazepine receptor, positive symptoms, schizophrenia.

## Introduction

An accumulating body of evidence has suggested that the pathophysiology of schizophrenia could be related to the dysregulation of the inflammatory response system, such as increased levels of *in vivo* IL-1RA, sIL-2R, and IL-6 (Lin *et al.* 1998; Nawa & Takei, 2006; Potvin *et al.* 2008; Zhang *et al.* 2004). Microglia has been regarded as a mediator of neuroinflammation via the release of pro-inflammatory cytokines, nitric oxide (NO) and reactive oxygen species (ROS) in the central nervous system (CNS). Peripheral benzodiazepine receptor (PBR) was reported to reflect neuronal injury and inflammatory lesions in the brain by increased expression of the number of binding sites in glial cells including activated microglia and reactive astrocytes as visualized *in vivo* using PET with [$^{11}$C]PK11195 (Shah *et al.* 1994). Recent reports demonstrated that [$^{11}$C]PK11195 binding was increased in patients with acute-onset schizophrenia (van Berckel *et al.* 2008) and in patients with schizophrenia during psychosis (Doorduin *et al.* 2009). However, the affinity (Chaki *et al.* 1999) and permeability of the blood–brain barrier was low for PK11195, reportedly a substrate of efflux transporter P-glycoprotein (Jakubikova *et al.* 2002; Vaalburg *et al.* 2005). Low uptake of [$^{11}$C]PK11195 in the brain could hamper stable quantitative analysis.

(*N*-5-fluoro-2-phenoxyphenyl)-*N*-(2,5-dimethoxylbenzyl) acetamide (DAA1106) is a potent and selective ligand for PBR with high affinity (Chaki *et al.* 1999; Okuyama *et al.* 1999). [$^{11}$C]DAA1106 is accumulated at high levels in the mouse brain (Zhang *et al.* 2003), and the radioactivity of [$^{11}$C]DAA1106 at 30 min after injection was reported to be four times higher than that of [$^{11}$C]PK11195 in the monkey brain (Maeda *et al.* 2004). A quantitative analysis method for [$^{11}$C]DAA1106 binding in the human brain has been well established with the two-tissue compartment model (Ikoma *et al.* 2007). [$^{11}$C]DAA1106 was

Address for correspondence: T. Suhara, M.D., Ph.D., Molecular Neuroimaging Group, Molecular Imaging Center, National Institute of Radiological Sciences, 4-9-1, Anagawa, Inage-ku, Chiba, 263-8555, Japan.
*Tel.*: +81-43-206-3251 *Fax*: +81-43-253-0396
*Email*: suhara@nirs.go.jp

**Table 1.** Demographic and clinical characteristics of the patients with schizophrenia

| Subject | Age (yr), sex | PANSS | | | | Duration of illness (yr) | Duration of drug treatment (yr) | Haloperidol equivalent (mg) | Main antipsychotics |
|---|---|---|---|---|---|---|---|---|---|
| | | Positive | Negative | General | Total | | | | |
| 1 | 29, F | 12 | 12 | 25 | 49 | 11 | 9 | 3 | Olanzapine |
| 2 | 34, F | 17 | 12 | 33 | 62 | 7 | 5 | 6 | Risperidone |
| 3 | 37, F | 14 | 23 | 27 | 64 | 0.5 | 0.5 | 3 | Olanzapine |
| 4 | 43, F | 21 | 27 | 49 | 97 | 22 | 19 | 17 | Risperidone |
| 5 | 46, F | 16 | 15 | 34 | 65 | 33 | 21 | 10 | Nemonapride |
| 6 | 49, F | 24 | 20 | 33 | 77 | 23 | 16 | 19.4 | Haloperidol |
| 7 | 42, M | 15 | 22 | 27 | 64 | 4 | 4 | 4 | Olanzapine |
| 8 | 43, M | 15 | 26 | 33 | 74 | 26 | 23 | 9 | Haloperidol |
| 9 | 44, M | 22 | 25 | 40 | 87 | 22 | 22 | 8.5 | Olanzapine |
| 10 | 44, M | 16 | 26 | 37 | 79 | 4 | 4 | 14 | Haloperidol |
| 11 | 46, M | 29 | 26 | 56 | 111 | 26 | 26 | 3.5 | Olanzapine |
| 12 | 46, M | 16 | 16 | 25 | 57 | 24 | 24 | 4 | Risperidone |
| 13 | 52, M | 24 | 35 | 58 | 117 | 18 | 17 | 16.5 | Olanzapine |
| 14 | 59, M | 27 | 24 | 47 | 87 | 43 | 39 | 10.3 | Mosapramine |
| | | $19.1 \pm 5.3$ | $22.1 \pm 6.5$ | $37.4 \pm 11.1$ | $77.9 \pm 20.1$ | $18.8 \pm 12.2$ | $16.4 \pm 10.8$ | $9.2 \pm 5.7$ | |

PANSS, Positive and Negative Syndrome Scale; F, female; M, male.
Haloperidol (1 mg) was equivalent to chlorpromazine (50 mg).

demonstrated to be useful in the study of neurodegerative disorders such as Alzheimer's disease (Yasuno *et al.* 2008).

In this study, we investigated PBR binding in patients with chronic schizophrenia using [$^{11}$C]DAA1106 to evaluate whether glial reaction was involved in the pathophysiology of schizophrenia.

## Materials and methods

### *Subjects*

Fourteen patients with schizophrenia [six females, eight males; $43.9 \pm 7.4$ yr (mean $\pm$ S.D.)] and 14 normal control subjects (five females, nine males; $42.5 \pm 9.0$ yr) were enrolled in this study. Patients were recruited from the outpatient and in-patient units of Nippon Medical School Hospital, Asai Hospital and Sobu Hospital, located in Tokyo and Chiba prefecture in Japan. The patients were diagnosed as having schizophrenia and treated by attending physicians at each hospital, and their diagnoses were re-evaluated with structured interviews at our PET centre. All 14 patients were diagnosed with schizophrenia according to DSM-IV criteria. Exclusion criteria were current or past substance, cannabis or alcohol abuse, mood disorders, and organic brain disease. The patients' demographic and clinical data are shown in Table 1. None of the patients had taken benzodiazepines within more than 1 month prior to PET measurements. Psychopathology was assessed by the Positive and Negative Syndrome Scale (PANSS; Kay *et al.* 1987). PANSS was completed by three experienced psychiatrists on the same day as the PET measurements. They reviewed the ratings after the interviews, and disagreements were resolved by consensus; the consensus ratings were used in this study. The symptom scores were calculated as total scores, positive symptom, negative symptom, and general symptom subscores of PANSS. The total PANSS score ranged from 49 to 117 ($78.6 \pm 20.7$). The mean positive symptom score was $19.1 \pm 5.3$, negative symptom score was $22.1 \pm 6.5$, and general symptom score was $37.4 \pm 11.1$.

The normal control subjects were recruited from the surrounding community. Based on psychiatric screening interviews, they were free of current and past psychiatric or major medical disease, and had no relatives with neuropsychiatric disorders.

This study complied with the current laws of Japan, and was approved by the Ethics and Radiation Safety Committee of the National Institute of Radiological Sciences, Chiba, Japan. Written informed consent was obtained from all subjects.

### *Radiochemistry*

[$^{11}$C]DAA1106 was prepared as described in detail previously (Ikoma *et al.* 2007; Zhang *et al.* 2003). The precursor was supplied by Taisho Pharmaceutical Co. (Japan).

### *PET data acquisition*

PET scans were performed with ECAT EXACT HR+ (CTI-Siemens, USA), which provides 63 planes and a 15.5-cm axial field of view (FOV). A 10-min transmission scan with a $^{68}$Ge–$^{68}$Ga source was followed by a 90-min dynamic scan (20s × 9, 60s × 5, 120s × 4, 240s × 11, and 300s × 6) with a bolus injection of 261–411 (369 ± 27) MBq of [$^{11}$C]DAA1106. Specific radioactivity was 15.4–220.7 GBq/$\mu$mol at the time of the injection. There was no significant difference in injected radioactivity and specific radioactivity between patients and normal controls (373 ± 20 MBq and 60.3 ± 44.4 GBq/$\mu$mol for patients, and 366 ± 32 MBq and 98.4 ± 70.7 GBq/$\mu$mol for normal controls). Radioactivity was measured in three-dimensional mode, and the data were reconstructed with a Hanning filter with a cut-off frequency of 0.4 (full width half maximum = 7.5 mm).

### Arterial blood sampling

To obtain the arterial input function, an automated blood sampling system was used for continuous (counts/s) blood radioactivity measurements during the first 12 min of PET measurement. At the same time, arterial blood samples were taken manually and their radioactivity concentration was measured 13 times during the initial 3 min after the injection, eight times during the next 17 min, and once every 10 min until the end of the scan. To analyse the metabolite fraction in the plasma, arterial blood samples were taken 10 times during PET measurements. The parent ligand, separated from the total radioactive compound, was measured as previously described (Ikoma *et al.* 2007). The mean time-course of the fraction of the parent ligand is shown in Fig. 1. There was a significant group × time interaction using repeated-measures ANOVA with Greenhouse–Geisser correction ($F_{3.4,81.1} = 4.92$, $p = 0.002$), although one subject from each group was excluded for the statistical analysis due to one missing data-point.

### *MR imaging*

T1-weighted magnetic resonance imaging (MRI) of the brain was performed with Philips Intera 1.5 T (Philips Medical Systems, The Netherlands). T1-weighted images of the brain were obtained from all subjects. The scan parameters were 1-mm-thick 3D T1 images with a transverse plane [repetition time (TR)/echo time (TE) 22/9.2 ms, flip angle 30°, matrix 128 × 128, FOV 256 × 256). Voxel size of the magnetic resonance images was 1 mm × 1 mm × 1 mm.

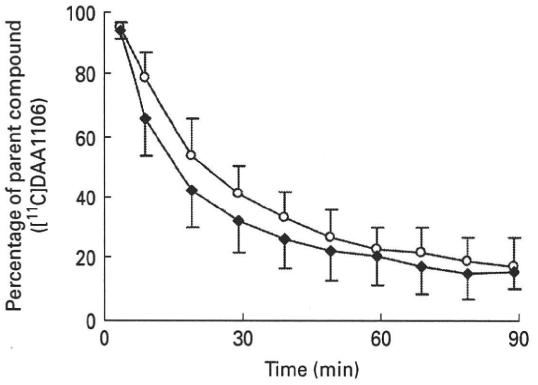


**Fig. 1.** Mean time-course of the percentage of parent compound ([$^{11}$C]DAA1106) after venous injection of [$^{11}$C]DAA1106 between normal controls (–○–) and patients (–◆–) with schizophrenia.

### Data analysis

Eleven regions of interest (ROIs) (medial frontal cortex, dorsolateral frontal cortex, medial temporal cortex, lateral temporal cortex, parietal cortex, occipital cortex, thalamus, striatum, cerebellum, anterior cingulate cortex, and posterior cingulate cortex) were delineated on the co-registered PET/MRI images. In addition to each regional ROI, eight cortical ROIs (medial frontal cortex, dorsolateral frontal cortex, medial temporal cortex, lateral temporal cortex, parietal cortex, occipital cortex, anterior cingulate cortex, and posterior cingulate cortex) were also summed up as total cortical regions.

Regional time–activity data were analysed with two-tissue compartment model (2-TC) with the metabolite-corrected plasma input function, a model demonstrated to estimate binding potential ($BP_{ND}$) most reliably for [$^{11}$C]DAA1106 (Ikoma *et al.* 2007). Rate constants were estimated with weighted least squares and the Marquardt optimizer. For each region, $k_1$, $k_2$, $k_3$, $k_4$ and blood volume were estimated by 2-TC. $BP_{ND}$ was calculated as $k_3/k_4$ in this analysis. Data analysis was performed with PMOD 2.65 (PMOD Technologies, Switzerland).

### Statistical analysis

#### *Regional ROIs*

Statistical analysis of the difference of regional $BP_{ND}$ for each ROI (for total 11 ROIs) between patients and normal controls was performed by repeated-measures ANOVA ($p < 0.05$ was considered significant). When any interaction was found, *post-hoc* Bonferroni correction was used for multiple comparisons.

**Table 2.** Significant correlation between PANSS scores and regional [$^{11}$C]DAA1106 binding

| PANSS scores | Region | *p* value |
|---|---|---|
| Positive symptom | Medial frontal cortex | 0.002* |
| | Dorsolateral frontal cortex | 0.022 |
| | Medial temporal cortex | 0.003* |
| | Lateral temporal cortex | 0.013 |
| | Parietal cortex | 0.005 |
| | Occipital cortex | 0.001* |
| | Cerebellum | 0.022 |
| | Striatum | 0.010 |
| Negative symptom | None | |
| General symptom | Medial frontal cortex | 0.018 |
| | Medial temporal cortex | 0.027 |
| | Occipital cortex | 0.038 |
| Total score | Medial frontal cortex | 0.012 |
| | Medial temporal cortex | 0.029 |
| | Parietal cortex | 0.044 |
| | Occipital cortex | 0.017 |

PANSS, Positive and Negative Syndrome Scale.
* $p < 0.0045$ (0.05/11).

Correlation between regional $BP_{ND}$ values and PANSS scores were analysed with Pearson's correlation method ($p < 0.05$ was considered significant).

Correlation between regional $BP_{ND}$ values and duration of illness, duration of drug treatment, and chlorpromazine equivalent doses (Inagaki *et al.* 1999) were analysed with Pearson's correlation method ($p < 0.05$ was considered significant).

Changes in regional $BP_{ND}$ values with age were analysed with Pearson's correlation method for patients and normal controls, respectively ($p < 0.05$ was considered significant).

### Total cortical regions

For analysing differences in total cortical regions between patients and normal controls, Student's *t* test was used ($p < 0.05$ was considered significant).

Correlations between $BP_{ND}$ values in total cortical regions and PANSS scores were analysed with Pearson's correlation method ($p < 0.05$ was considered significant).

Correlation between $BP_{ND}$ values in total cortical regions and duration of illness, duration of drug treatment, and chlorpromazine-equivalent doses (Inagaki *et al.* 1999) were analysed with Pearson's correlation method ($p < 0.05$ was considered significant).

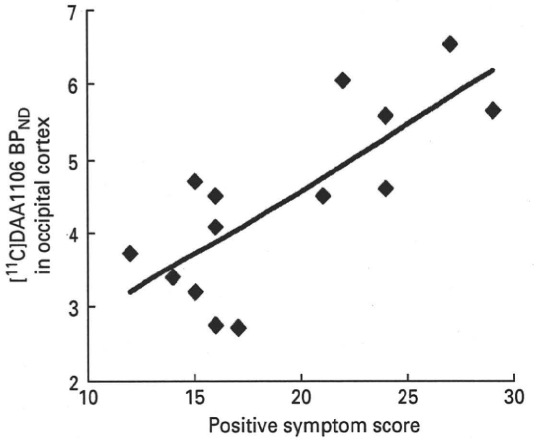


**Fig. 2.** Positive correlation between [$^{11}$C]DAA1106 $BP_{ND}$ in the occipital cortex and positive symptom scores in the Positive and Negative Syndrome Scale.

Changes in $BP_{ND}$ values in total cortical regions with age were analysed with Pearson's correlation method for patients and normal controls, respectively ($p < 0.05$ was considered significant).

## Results

### *Regional ROIs*

Comparison of regional $BP_{ND}$ values for [$^{11}$C]DAA1106 between the patients with schizophrenia and normal controls by two-way repeated ANOVA with Greenhouse–Geisser correction showed no significant group × region interaction ($F_{1.7,44.4} = 0.542$, $p = 0.558$).

For the correlation analysis between $BP_{ND}$ values in regional ROIs and positive symptom scores in the patient group, significant correlations were found in regions such as the medial frontal cortex, medial temporal cortex and occipital cortex (Table 2) (Fig. 2). No correlation was found between $BP_{ND}$ values of each region and negative symptoms. Those three regions showed trends of positive correlation with general symptoms and total score (Table 2). There was no significant correlation between regional $BP_{ND}$ and the duration of illness.

There was no significant change of regional $BP_{ND}$ values with age in normal controls, whereas significant changes in $BP_{ND}$ values with age in the patients with schizophrenia were observed in the occipital cortex ($p = 0.014$), lateral temporal cortex ($p = 0.023$), parietal cortex ($p = 0.023$), medial temporal cortex ($p = 0.031$), and medial frontal cortex ($p = 0.036$).

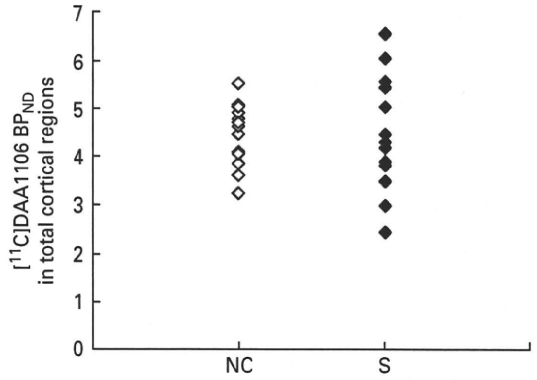


**Fig. 3.** Comparison of [$^{11}$C]DAA1106 $BP_{ND}$ of total cortical regions between normal controls (NC) and patients with schizophrenia (S).

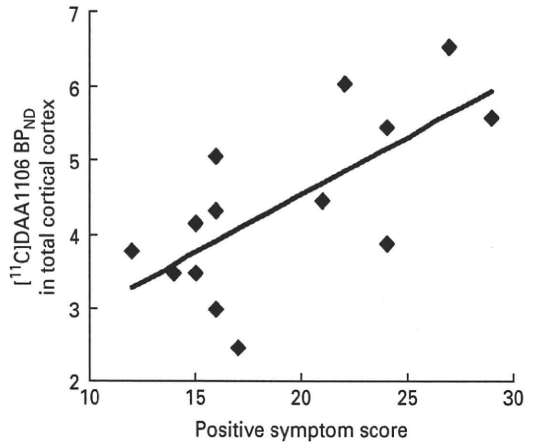


**Fig. 4.** Positive correlation between [$^{11}$C]DAA1106 $BP_{ND}$ in the total cortical region and positive symptom scores in the Positive and Negative Syndrome Scale.

### *Total cortical regions*

There was no significant difference of $BP_{ND}$ values in total cortical regions between patients with schizophrenia and normal controls (Fig. 3). Significant correlation was found with the positive symptom scores ($p=0.006$) (Fig. 4). There was no significant correlation with other symptom scores (negative, general, and total symptom scores). Total cortical regions were correlated with duration of illness ($p=0.020$) (Fig. 5) and duration of drug treatment ($p=0.023$). $BP_{ND}$ of total cortical regions was not correlated with chlorpromazine-equivalent doses.

There was no significant change of $BP_{ND}$ values in total cortical regions with age in normal controls, but significant changes of $BP_{ND}$ values with age were observed in total cortical regions of the patients with schizophrenia ($p=0.018$).

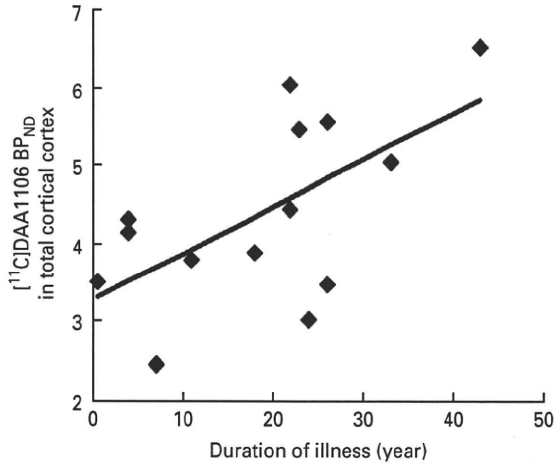


**Fig. 5.** Positive correlation between [$^{11}$C]DAA1106 $BP_{ND}$ in the total cortical region and duration of illness.

## Discussion

In this study, [$^{11}$C]DAA1106 binding, which was considered to correspond to the density of PBR, was not different between the patients with chronic schizophrenia and normal controls. A recent study demonstrated that [$^{11}$C]PK11195 binding increased in total grey matter in patients with acute-onset schizophrenia (van Berckel *et al.* 2008). Another recent study reported that [$^{11}$C]PK11195 binding in the hippocampus was significantly increased in patients with schizophrenia during acute psychosis, while there was no significant difference in other regions compared with normal controls (Doorduin *et al.* 2009). To understand the difference in the results between the present study and the two [$^{11}$C]PK11195 studies, several factors, such as the use of different radioligands and different patient groups, should be taken into consideration. Although PK11195 fully displaced the [$^{3}$H]DAA1106 binding (Chaki *et al.* 1999), a high concentration of PK11195 was required for this displacement. This suggested that the binding domain for DAA1106 contains an extra component that does not interact efficiently with PK11195 (Chaki *et al.* 1999). The mean age of patients with schizophrenia enrolled in the present study was higher (44 yr in 14 patients) than those in the two [$^{11}$C]PK11195 studies (24 yr in 10 patients, and 31 yr in seven patients). Most of the patients in the present study were at the chronic stage.

Within the patient group, [$^{11}$C]DAA1106 binding had a significant correlation with the positive symptom score of PANSS, a finding that might be in line

with those recent findings with [$^{11}$C]PK11195. The present results might indicate that the activated neuroimmune system was related to the pathophysiology of schizophrenia at the chronic stage.

In previous MRI volumetric research in schizophrenia, volume reduction in the brain has been reported in patients with chronic schizophrenia (Shenton *et al.* 2001). However, in the present study, there was no significant difference in the volume of ROIs by ANOVA, and total cortical ROI by Student's *t* test between the patients and normal controls (data not shown). Thus, the insignificance of the difference of [$^{11}$C]DAA1106 binding between the patients and normal controls is not related to the partial volume effect due to brain atrophy.

In this study, normal controls showed no age effects on [$^{11}$C]DAA1106 binding in any region. This is in line with the report with [$^{11}$C]PK11195 binding except the thalamus, where [$^{11}$C]PK11195 binding was reported to increase with age (Cagnin *et al.* 2001). This might be due to different radioligands or different age ranges between the two studies (24–55 yr in this study and 32–80 yr in the [$^{11}$C]PK11195 study). On the other hand, [$^{11}$C]DAA1106 binding was found to increase with age in patients with schizophrenia. Schizophrenia has been considered to be progressive in functional disability and morphological changes (Lieberman *et al.* 2001; Mathalon *et al.* 2001; Saijo *et al.* 2001). The present results of the positive correlation among [$^{11}$C]DAA1106 binding, duration of illness, and age might suggest that the progressive change occurs at the glial reaction level.

A recent meta-analysis showed that some cytokines such as IL-1RA, sIL-2R, and IL-6 are increased in schizophrenia (Potvin *et al.* 2008). PBR has been considered to modulate the release of pro-inflammatory cytokines in the CNS. PBR was reported to modulate the release of the inflammatory molecules NO and tumour necrosis factor-alpha (TNF-$\alpha$) (Wilms *et al.* 2003). A PBR ligand, PK11195, has been reported to inhibit lipopolysaccharide-induced expressions of COX-2 and TNF-$\alpha$ in human microglia (Choi *et al.* 2002). Immunomodulatory drugs such as cyclooxygenase-2 (COX-2) inihibitors have been reported to show beneficial effects in schizophrenia (Muller & Schwarz, 2008). The combination of risperidone and COX-2 inhibitor has been reported to show superiority over risperidone alone in positive symptoms and PANSS total scores (Akhondzadeh *et al.* 2007). On the other hand, cytokines such as IL-2 and IL-6 are reported to increase after olanzapine and clozapine treatment (Kluge *et al.* 2009). The present results of PBR binding in the patients with schizophrenia might be in accord with the previous reports of cytokines.

A recent report demonstrated that PBR expression was not confined to microglia but was inducible in nervous tissue cells of neuroepithelial origin (Ji *et al.* 2008). Thus, PBR binding might also arise from astrocytes and other non-microglial elements. Schizophrenia patients with high S100B serum concentration, considered to indicate astrocyte activation, were reported to have cognitive dysfunction compared with patients with low S100B serum concentration (Pedersen *et al.* 2008). DAA1106 binding in patients with schizophrenia might also be related to the change in PBR on astrocytes.

In a post-mortem study, a subgroup of the patients with schizophrenia who committed suicide had increased microglial densities, although microglial HLA-DR expression in the patients with schizophrenia was not different from normal controls (Steiner *et al.* 2008). Microglial activation has been suggested to be interpretable as a consequence of presuicidal stress (Avital *et al.* 2001; Lehmann *et al.* 2002).

Although $BP_{ND}$ of total cortical regions was not correlated with chlorpromazine-equivalent doses in the present study, some antipsychotics were reported to have anti-inflammatory effects (Kato *et al.* 2007; Kowalski *et al.* 2003, 2004; Labuzek *et al.* 2005; Zheng *et al.* 2008). The effect of antipsychotics on DAA1106 binding remains to be studied.

There are several confounding factors in the present study. First, the number of subjects was relatively small. Further larger-scale studies will be needed to confirm the present results. Second, all the patients were under different kinds of antipsychotic treatment. Further study is needed with drug-naive patients and patients under well-controlled drug treatment. Third, the PANSS scores of patients were higher as the duration of the illness was longer and age increased. This might reflect a possible subgroup of treatment-resistant patients.

In conclusion, we found no significant differences in PBR binding between the brains of patients with schizophrenia and those of normal control subjects, unlike recent reports with [$^{11}$C]PK11195 (van Berckel *et al.* 2008; Doorduin *et al.* 2009). Nevertheless, PBR binding in the patients with schizophrenia was correlated with positive symptoms, disease duration and age. The present results suggest that the glial reaction process might be involved in the pathophysiology of schizophrenia. Although the correlations should be interpreted with caution, these results at least suggest that additional studies are warranted in order to determine whether baseline

differences exist between patients with schizophrenia and healthy subjects, as well as to reveal the biological meanings of the correlations with disease parameters.

### Acknowledgments

This work was supported in part by the Ministry of Education, Culture, Sports, Science and Technology, Grant-in-Aid for Young Scientists (B) (16790710, 2004–2005), and a consignment expense for the Molecular Imaging Program on 'Research Base for PET Diagnosis' from the Ministry of Education, Culture, Sports, Science and Technology (MEXT), Japanese Government.

### Statement of Interest

None.

### References

**Akhondzadeh S, Tabatabaee M, Amini H, Ahmadi Abhari SA, *et al.*** (2007). Celecoxib as adjunctive therapy in schizophrenia: a double-blind, randomized and placebo-controlled trial. *Schizophrenia Research* **90**, 179–185.

**Avital A, Richter-Levin G, Leschiner S, Spanier I, *et al.*** (2001). Acute and repeated swim stress effects on peripheral benzodiazepine receptors in the rat hippocampus, adrenal, and kidney. *Neuropsychopharmacology* **25**, 669–678.

**Cagnin A, Brooks DJ, Kennedy AM, Gunn RN, *et al.*** (2001). In-vivo measurement of activated microglia in dementia. *Lancet* **358**, 461–467.

**Chaki S, Funakoshi T, Yoshikawa R, Okuyama S, *et al.*** (1999). Binding characteristics of [$^{3}$H]DAA1106, a novel and selective ligand for peripheral benzodiazepine receptors. *European Journal of Pharmacology* **371**, 197–204.

**Choi HB, Khoo C, Ryu JK, van Breemen E, *et al.*** (2002). Inhibition of lipopolysaccharide-induced cyclooxygenase-2, tumor necrosis factor-alpha and $[Ca^{2+}]_i$ responses in human microglia by the peripheral benzodiazepine receptor ligand pK11195. *Journal of Neurochemistry* **83**, 546–555.

**Doorduin J, de Vries EF, Willemsen AT, de Groot JC, *et al.*** (2009). Neuroinflammation in schizophrenia-related psychosis: a pET study. *Journal of Nuclear Medicine* **50**, 1801–1807.

**Ikoma Y, Yasuno F, Ito H, Suhara T, *et al.*** (2007). Quantitative analysis for estimating binding potential of the peripheral benzodiazepine receptor with [$^{11}$C]DAA1106. *Journal of Cerebral Blood Flow and Metabolism* **27**, 173–184.

**Inagaki A, Inada T, Fujii Y, Gohei Y, *et al.*** (1999). *Equivalent Doses of Antipsychotic Medications* [in Japanese]. Tokyo: Seiwa Press.

**Jakubikova J, Duraj J, Hunakova L, Chorvath B, *et al.*** (2002). PK11195, an isoquinoline carboxamide ligand of the mitochondrial benzodiazepine receptor, increased drug uptake and facilitated drug-induced apoptosis in human multidrug-resistant leukemia cells in vitro. *Neoplasma* **49**, 231–236.

**Ji B, Maeda J, Sawada M, Ono M, *et al.*** (2008). Imaging of peripheral benzodiazepine receptor expression as biomarkers of detrimental *vs.* beneficial glial responses in mouse models of alzheimer's and other cNS pathologies. *Journal of Neuroscience* **28**, 12255–12267.

**Kato T, Monji A, Hashioka S, Kanba S** (2007). Risperidone significantly inhibits interferon-gamma-induced microglial activation in vitro. *Schizophrenia Research* **92**, 108–115.

**Kay SR, Fiszbein A, Opler LA** (1987). The positive and negative syndrome scale (PANSS) for schizophrenia. *Schizophrenia Bulletin* **13**, 261–276.

**Kluge M, Schuld A, Schacht A, Himmerich H, *et al.*** (2009). Effects of clozapine and olanzapine on cytokine systems are closely linked to weight gain and drug-induced fever. *Psychoneuroendocrinology* **34**, 118–128.

**Kowalski J, Labuzek K, Herman ZS** (2003). Flupentixol and trifluperidol reduce secretion of tumor necrosis factor-alpha and nitric oxide by rat microglial cells. *Neurochemistry International* **43**, 173–178.

**Kowalski J, Labuzek K, Herman ZS** (2004). Flupentixol and trifluperidol reduce interleukin-1 beta and interleukin-2 release by rat mixed glial and microglial cell cultures. *Polish Journal of Pharmacology* **56**, 563–570.

**Labuzek K, Kowalski J, Gabryel B, Herman ZS** (2005). Chlorpromazine and loxapine reduce interleukin-1beta and interleukin-2 release by rat mixed glial and microglial cell cultures. *European Neuropsychopharmacology* **15**, 23–30.

**Lehmann J, Weizman R, Leschiner S, Feldon J, *et al.*** (2002). Peripheral benzodiazepine receptors reflect trait (early handling) but not state (avoidance learning). *Pharmacology Biochemistry and Behavior* **73**, 87–93.

**Lieberman J, Chakos M, Wu H, Alvir J, *et al.*** (2001). Longitudinal study of brain morphology in first episode schizophrenia. *Biological Psychiatry* **49**, 487–499.

**Lin A, Kenis G, Bignotti S, Tura GJ, *et al.*** (1998). The inflammatory response system in treatment-resistant schizophrenia: increased serum interleukin-6. *Schizophrenia Research* **32**, 9–15.

**Maeda J, Suhara T, Zhang MR, Okauchi T, *et al.*** (2004). Novel peripheral benzodiazepine receptor ligand [11C]DAA1106 for pET: an imaging tool for glial cells in the brain. *Synapse* **52**, 283–291.

**Mathalon DH, Sullivan EV, Lim KO, Pfefferbaum A** (2001). Progressive brain volume changes and the clinical course of schizophrenia in men: a longitudinal magnetic resonance imaging study. *Archives of Genenal Psychiatry* **58**, 148–157.

**Muller N, Schwarz MJ** (2008). COX-2 inhibition in schizophrenia and major depression. *Current Pharmaceutical Design* **14**, 1452–1465.

**Nawa H, Takei N** (2006). Recent progress in animal modeling of immune inflammatory processes in schizophrenia: implication of specific cytokines. *Neuroscience Research* **56**, 2–13.

**Okuyama S, Chaki S, Yoshikawa R, Ogawa S, *et al.*** (1999). Neuropharmacological profile of peripheral benzodiazepine receptor agonists, dAA1097 and dAA1106. *Life Science* **64**, 1455–1464.

**Pedersen A, Diedrich M, Kaestner F, Koelkebeck K, *et al.*** (2008). Memory impairment correlates with increased s100B serum concentrations in patients with chronic schizophrenia. *Progress in Neuro-psychopharmacology and Biological Psychiatry* **32**, 1789–1792.

**Potvin S, Stip E, Sepehry AA, Gendron A, *et al.*** (2008). Inflammatory cytokine alterations in schizophrenia: a systematic quantitative review. *Biological Psychiatry* **63**, 801–808.

**Saijo T, Abe T, Someya Y, Sassa T, *et al.*** (2001). Ten year progressive ventricular enlargement in schizophrenia: an mRI morphometrical study. *Psychiatry and Clinical Neuroscience* **55**, 41–47.

**Shah F, Hume SP, Pike VW, Ashworth S, *et al.*** (1994). Synthesis of the enantiomers of [*N*-methyl-$^{11}$C]PK 11195 and comparison of their behaviours as radioligands for pK binding sites in rats. *Nuclear Medicine and Biology* **21**, 573–581.

**Shenton ME, Dickey CC, Frumin M, McCarley RW** (2001). A review of mRI findings in schizophrenia. *Schizophrenia Research* **49**, 1–52.

**Steiner J, Bielau H, Brisch R, Danos P, *et al.*** (2008). Immunological aspects in the neurobiology of suicide: elevated microglial density in schizophrenia and depression is associated with suicide. *Journal of Psychiatric Research* **42**, 151–157.

**Vaalburg W, Hendrikse NH, Elsinga PH, Bart J, *et al.*** (2005). P-glycoprotein activity and biological response. *Toxicology and Applied Pharmacology* **207**, 257–260.

**van Berckel BN, Bossong MG, Boellaard R, Kloet R, *et al.*** (2008). Microglia activation in recent-onset schizophrenia: a quantitative (R)-[$^{11}$C]PK11195 positron emission tomography study. *Biological Psychiatry* **64**, 820–822.

**Wilms H, Claasen J, Rohl C, Sievers J, *et al.*** (2003). Involvement of benzodiazepine receptors in neuroinflammatory and neurodegenerative diseases: evidence from activated microglial cells in vitro. *Neurobiology of Disease* **14**, 417–424.

**Yasuno F, Ota M, Kosaka J, Ito H, *et al.*** (2008). Increased binding of peripheral benzodiazepine receptor in alzheimer's disease measured by positron emission tomography with [$^{11}$C]DAA1106. *Biological Psychiatry* **64**, 835–841.

**Zhang MR, Kida T, Noguchi J, Furutsuka K, *et al.*** (2003). [$^{11}$C]DAA1106: radiosynthesis and in vivo binding to peripheral benzodiazepine receptors in mouse brain. *Nuclear Medicine and Biology* **30**, 513–519.

**Zhang XY, Zhou DF, Cao LY, Zhang PY, *et al.*** (2004). Changes in serum interleukin-2, -6, and -8 levels before and during treatment with risperidone and haloperidol: relationship to outcome in schizophrenia. *Journal of Clinical Psychiatry* **65**, 940–947.

**Zheng LT, Hwang J, Ock J, Lee MG, *et al.*** (2008). The antipsychotic spiperone attenuates inflammatory response in cultured microglia via the reduction of proinflammatory cytokine expression and nitric oxide production. *Journal of Neurochemistry* **107**, 1225–1235.